

UC San Diego

UC San Diego Electronic Theses and Dissertations

Title

Mars Rover : laser focusing and optimization

Permalink

<https://escholarship.org/uc/item/6jz7f8s6>

Author

Barkley, Walter Clifford

Publication Date

2008

Peer reviewed|Thesis/dissertation

UNIVERSITY OF CALIFORNIA, SAN DIEGO

Mars Rover - Laser Focusing and Optimization

A Thesis submitted in partial satisfaction of the requirements
for the degree Master of Science

in

Engineering Sciences (Mechanical Engineering)

by

Walter Clifford Barkley

Committee in charge:

Professor Miroslav Krstic, Chair
Professor Thomas Bewley
Professor William Hodgkiss

2008

Copyright

Walter Clifford Barkley, 2008

All rights reserved.

The thesis of Walter Clifford Barkley is approved and is acceptable in quality and form for publication on microfilm and electronically:

Chair

University of California, San Diego

2008

TABLE OF CONTENTS

Signature Page.....	iii
Table of Contents	iv
List of Figures	v
List of Tables.....	vii
Abstract	viii
Introduction	1
Chapter 1 - The Secondary Mirror Slider Mechanism	8
Chapter 2 - Focusing Methods	13
Method 1 – Hunt Through Entire Range	13
Method 2 – Hunt Through Camera Determined Distance Range of $d \pm 0.05d$	13
Method 3 – Hunt Partially Through Camera Determined Distance Range.....	13
Chapter 3 - Engineering Model Experiments, Data and Analysis	16
Experiment Number 1	16
Experiment Number 2	31
Chapter 4 - Signal Processing and Optimization.....	36
Option 1 – White Noise	38
Option 2 – Colored Noise	40
Chapter 5 - Signal Optimization and Computational Analysis.....	42
Conclusion.....	44
Appendix A	45
Appendix B	46
Appendix C	51
References	56

LIST OF FIGURES

Figure 1 – Artist’s Rendition of the Mars Scientific Laboratory Rover [3]	2
Figure 2 - ChemCam Mast Unit	3
Figure 3 – Pictorial Layout of ChemCam Mast and Body Units.....	3
Figure 4 – Secondary Mirror Slider Mechanism	8
Figure 5 – Motor Steps versus Target Distance Using Data Developed by the French Team.....	9
Figure 6 – Motor Step Increment Determination Chart.....	10
Figure 7 - Logic Flowchart for Focusing and Optimizing the LIBS Laser on Target, Target Distance Known	15
Figure 8 – Prototype ChemCam Instrument Mast Unit (Engineering Model)	16
Figure 9 – Spectra Composite of 12 Laser Shots at 1.5 m Target Distance	19
Figure 10 – Spectra Composite of 3 Laser Shots at 3 m Target Distance	19
Figure 11 – Spectra Composite of 9 Laser Shots at 5 m Target Distance	20
Figure 12 – Spectra Composite of 6 Laser Shots at 7 m Target Distance	20
Figure 13 – Spectra Composite of 10 Laser Shots at 9 m Target Distance	21
Figure 14 – Ultraviolet Light Spectra at 1.5 Meters, Shots 1 through 3.....	22
Figure 15 – Ultraviolet Light Spectra at 1.5 Meters, Shots 4 through 6.....	23
Figure 16 – Ultraviolet Light Spectra at 1.5 Meters, Shots 7 through 9.....	23
Figure 17 – Ultraviolet Light Spectra at 1.5 Meters, Shots 10 through 12.....	24
Figure 18 – Visible Light Spectra at 1.5 Meters, Shots 1 through 3.....	24
Figure 19 – Visible Light Spectra at 1.5 Meters, Shots 4 through 6.....	25
Figure 20 – Visible Light Spectra at 1.5 Meters, Shots 7 through 9.....	25
Figure 21 – Visible Light Spectra at 1.5 Meters, Shots 10 through 12.....	26
Figure 22 – Ultraviolet Light Spectrum at 1.5 Meters (8th Shot).....	26
Figure 23 – Visible Light Spectrum at 1.5 Meters (8th Shot)	27
Figure 24 – Ultraviolet and Visible Light Spectra at 9 Meters (1st through 3rd Shots).....	28
Figure 25 – Ultraviolet and Visible Light Spectra at 9 Meters (4th through 6th Shots).....	29

Figure 26 – Ultraviolet and Visible Light Spectra at 9 Meters (7th through 9th Shots).....	29
Figure 27 – Background Number 1 at 2m.....	32
Figure 28 – Sample Number 1 at 2m.....	32
Figure 29 – Background Number 4 at 2m.....	33
Figure 30 – Sample Number 4 at 2m.....	33
Figure 31 – Background Number 7 at 2m.....	34
Figure 32 – Sample Number 7 at 2m.....	34
Figure 33 – Background Number 9 at 2m.....	35
Figure 34 – Sample Number 9 at 2m.....	35
Figure 35 – Histograms of 50 Test Statistics: Sample 7 and Background vnir Spectrometers; Data from Experiment 2.....	39
Figure 36 – Histograms of 50 Test Statistics: Sample 7 and Background vis Spectrometers; Data from Experiment 2.....	41

LIST OF TABLES

Table 1 – Constants Used in Equation 1	4
Table 2 - Spectral Range of Spectrometers	4
Table 3 – Mars Data [5]	5
Table 4 – Statistical Signal Processing Decision Matrix	6
Table 5 - Laser Focusing Statistics	12
Table 6 – Increment Experiment Data	18
Table 7 – Chemical Composition of Aluminum 6061	30
Table 8 – Main Lines in Atomic Spectrum of Aluminum 6061 [6]	30
Table 9 - Samples Used for Experiment 2 [7]	31

ABSTRACT OF THE THESIS

Mars Rover – Laser Focusing and Optimization

by

Walter Clifford Barkley

Master of Science in Engineering Sciences (Mechanical Engineering)

University of California, San Diego, 2008

Professor Miroslav Krstic, Chair

This thesis was initiated through the requirements of the ChemCam instrument team at Los Alamos National Laboratory to obtain a backup method for focusing a laser on the 2009 Mars Scientific Laboratory (MSL) rover. The ChemCam instrument uses Laser-Induced Breakdown Spectroscopy (LIBS) to analyze the chemical composition of material on the Martian surface.

The primary focus system uses a laser range-finder, charge-coupled device (CCD) and auto-focusing algorithm to focus the LIBS laser. The backup system, developed in this project, employs signal processing and optimization techniques to mitigate the risk of an inoperable instrument due to range-finder failure. These techniques have resulted in the development of algorithms and software code listed in Appendices B and C which can be loaded on the rover's computer before launch or uploaded from Mission Control to the Mars rover after arrival.

The scope of this work is limited to: focusing algorithm for the LIBS laser to produce plasma on target and optimizing the laser focal length to maximize the intensity of light signal returning from the plasma. A range of signal processing techniques are considered and a one-dimensional optimization is implemented.

Introduction

A series of missions to Mars is being executed by the National Aeronautics and Space Administration (NASA) and managed by the Jet Propulsion Laboratory (JPL) in Pasadena, California. Scheduled to launch in the fall of 2009, MSL is a rover that will assess a variety of scientific objectives, including whether Mars ever was, or is still today, an environment able to support microbial life. The MSL rover will carry the biggest, most advanced suite of instruments for scientific studies ever sent to the Martian surface [1]. These instruments capture data that is sent back to Earth to study the elemental composition of rock, soil and ice on the planet surface. One of the instruments, ChemCam is developed by Los Alamos National Laboratory (LANL) and Centre d'Etude Spatiale des Rayonnements (CESR, France) for JPL.

ChemCam will identify surface elements by combining Laser-Induced Breakdown Spectroscopy (LIBS) [2] with a Remote Micro-Imager (RMI) to provide spectra and images of the target. LIBS is a type of atomic emission spectroscopy which utilizes a highly energetic laser pulse as the excitation source. Because all elements emit light when excited to sufficiently high temperatures, LIBS can detect all elements, limited only by the power of the laser as well as the sensitivity and wavelength range of the spectrograph and detector. Operationally, LIBS is very similar to arc/spark emission spectroscopy.

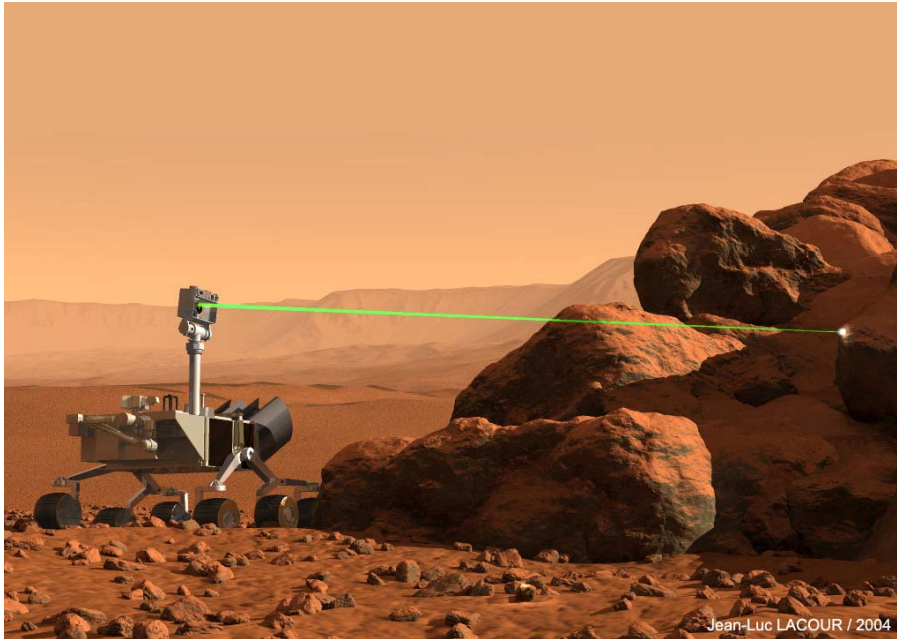


Figure 1 – Artist's Rendition of the Mars Scientific Laboratory Rover [3]

Modeled in Figure 1, the MSL rover deploys the ChemCam apparatus on a mast to fire the LIBS laser on a target. The laser light is fired out of the telescope lens in a conical shape that is focused down to a spot at the target. Cameras aboard the rover triangulate the target distance to within $\pm 5\%$ and a Continuous-Wave Laser (CWL, Figure 2) housed in the ChemCam instrument further refines the target range to $\pm 0.5\%$. Once the target distance is windowed, an auto-focus algorithm (developed by CESR) is initiated to position the optics for focal point on target. The focusing is performed by commanding a motor-driven linear sliding mechanism that adjusts the secondary mirror (SM) position in the telescope (Figures 2 and 3).

The diagram illustrates the LIBS system architecture, divided into two main sections: the **Mast** and the **Body**.

Mast Section:

- Remote Micro-Imager (RMI):** Located at the top of the mast.
- Front-End Electronics:** Positioned below the RMI.
- Laser:** A red box on the left that emits a laser beam through a mirror and lens system into the telescope.
- Telescope:** A large blue trapezoidal structure that focuses the laser beam and collects light from the target.
- Spark light:** A small yellow starburst representing the laser-induced plasma on the target.
- LIBS Target is 1-9 m Away:** A dark, rocky sphere representing the target.

Body Section:

- Optical Fibers:** A bundle of fibers that transmit light from the telescope to the spectrographs.
- MUX (Multiplexer):** A small blue box that directs light from the fibers into the spectrographs.
- Spectrographs (3):** Three yellow rectangular units that analyze the light spectrum.
- CCD (Charge-Coupled Device):** A component within the spectrographs that captures the spectral data.
- Processing:** A vertical yellow box that handles the data from the CCD.
- Power Converter:** A yellow box that converts power for the system.
- CPU (Central Processing Unit):** A large yellow box that manages the system's operations.
- Rover Interface (RS-422):** A yellow box that facilitates communication between the rover and the LIBS system.
- External Connections:** Arrows indicate connections for **Command**, **Telemetry**, and **Power** to the Rover Interface.

The **Rover Mast** is shown at the bottom left, with **azimuth** and **elevation** adjustment mechanisms.

Figure 3 – Pictorial Layout of ChemCam Mast and Body Units

When the high-powered, LIBS laser is focused and fired on a target, the intense heat causes a change of state of the elements, which creates plasma. The light emitted from the plasma is collected by the telescope in the Mast Unit and injected into an optical fiber that transports the light signal to three spectrometers: ultraviolet (uv), visible (vis) and very near infrared (vnir) that are housed in the Body Unit (Figure 3). These spectrometers are charge-coupled devices (CCD's) that capture light in 2,048 columns of pixels corresponding to wavelengths according to equation 1:

$$w = C_0 + C_1i + C_2i^2 + C_3i^3 \quad (1)$$

where w is the wavelength in nanometers, C_x are constants defined in Table 1 and i is the index. The pairing of these wavelengths to the ChemCam output data yields the graphical representation of light intensity versus wavelength for each spectrograph.

Table 1 – Constants Used in Equation 1

Spectrometer	Index Start Point	C_0	C_1	C_2	C_3
VNIR	50	4.02E+02	2.21E-01	-3.32E-06	-1.27E-09
VIS	2198	3.13E+02	1.83E-02	8.49E-06	-9.25E-10
UV	4346	-5.59E+01	9.17E-02	-6.67E-06	3.29E-10

Equation 1 produces a set of 2048 points for each of the spectrometers at the wavelength ranges shown in Table 2:

Table 2 - Spectral Range of Spectrometers

uv	243.5 → 343.5 nm
vis	384.9 → 473.5 nm
vnir	413.0 → 839.6 nm

By analyzing the peaks of the data output from the spectrographs and their associated wavelengths, individual elements can be identified from their spectral

signature. When all of the elements in the light sample are identified from the spectrometers, the composition of the target material can be determined. The rover's on-board computer transmits the data back to Earth where the analysis is performed.

The objective of this thesis project is to provide an alternative method to focus the LIBS laser if the CWL fails. This result is met by providing software code and algorithms detailed in Appendices B and C.

Before proceeding, some important Mars data is summarized in Table 3:

Table 3 – Mars Data [5]

Rotation Period	24.66 hours
Orbital Period	1.88 years
Inclination of Equator to Orbit	25.19°
Mass (Earth = 1)	0.107
Surface Gravity (Earth = 1)	0.379
Surface Temperatures: Maximum, Minimum	-5°C, -87°C
Atmosphere	95.32% CO ₂
Atmospheric Pressure	0.0063 atm

Referring to Table 3, the rotational period on Mars is 24.66 hours, very close to an Earth day. The inclination of the equator to orbit of 25.19° is close to Earth's 23.45°. Because of these facts, the length of the day on Mars (sol) will depend on the season and on the location of the rover in either the northern or southern hemisphere (the landing site of the MSL on Mars has not yet been decided). ChemCam can be operated during the day or night on Mars.

The ChemCam instrument is exposed to background light from the sun during daytime operations and this light is considered noise for the purpose of laser focusing. Characterizing the noise prior to firing the LIBS laser allows the creation of statistical metrics particular to the current light environment: mean, standard deviation and variance

are computed for all measureable wavelengths. Statistical signal processing techniques are used to make a decision whether or not plasma light signal is present in the noise (Table 4):

Table 4 – Statistical Signal Processing Decision Matrix

	Decision	
Truth	D_0	D_1
\mathcal{H}_0	P_{CR}	P_{FA}
\mathcal{H}_1	P_M	P_D

where \mathcal{H}_0 is the hypothesis of noise only, \mathcal{H}_1 is the hypothesis of noise plus signal; D_0 is the decision of noise without signal, D_1 is the decision of noise with signal, P_{CR} is the probability of a correct rejection, P_{FA} is the probability of a false alarm detection, P_M is the probability of a missed detection and P_D is the probability of a correct detection. These probabilities can be computed directly from the measured data which will be described in Chapter 4.

Chapter 1 details the mechanism for focusing the laser and the mathematical relationship between motor steps and laser focus distance. Chapter 2 describes methods to focus the laser on a target and selects the best method to pursue in this project. A flowchart is presented that pictorially depicts the logic followed to construct the code written in Appendices B and C. Chapter 3 presents data and analysis obtained from two lab experiments performed at Los Alamos National Laboratory on prototype flight hardware. The experiments are used to develop the strategy for background light reference data, thresholds and test statistics for signal detection. Conclusions on the viability of the signal detection and optimization methods are discussed. Chapter 4 applies advanced signal processing techniques used to characterize the noise and to detect

the signal in noise that is central to efficient use of the instrument. Probability density functions and their graphical representation are shown to illustrate the techniques. The probabilities of detection and of false alarm are illustrated and the one-dimensional maximization equation is described. The appendices follow.

Chapter 1 - The Secondary Mirror Slider Mechanism

The Secondary Mirror Slider Mechanism (Figure 4) is used to focus the LIBS laser on target. The stepper motor positions the mirror through a total slide length of 13 mm. The SM focus position farthest away from the motor focuses the laser down to a target distance of 1.5 m and the SM position closest to the motor focuses the laser to a target distance of 9 m. There is a SM position called “sun-safe” that protects the optics from the sun and is located beyond the 1.5 m focus position. Also, there are position sensors and hard stops at both ends of the slider range; however, the motor does not have an encoder to provide direct position feedback to the control system.

Through research done in France, the French Team at CESR developed a relationship between slider mechanism motor steps and target distance (Figure 5). For a given target distance, the relationship established in Figure 5 is used to position the secondary mirror for optimum laser focus.

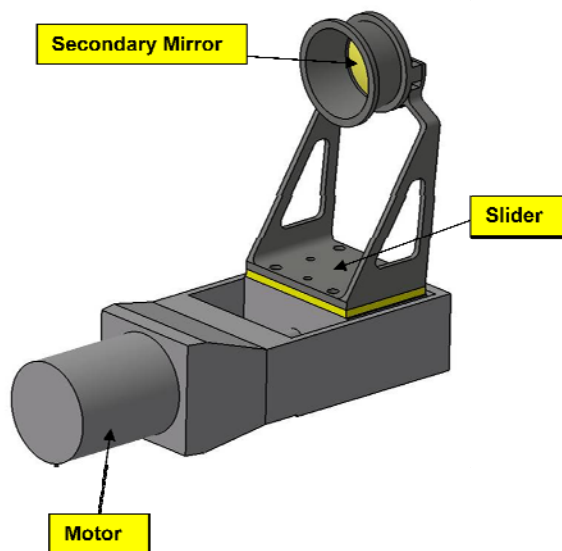


Figure 4 – Secondary Mirror Slider Mechanism

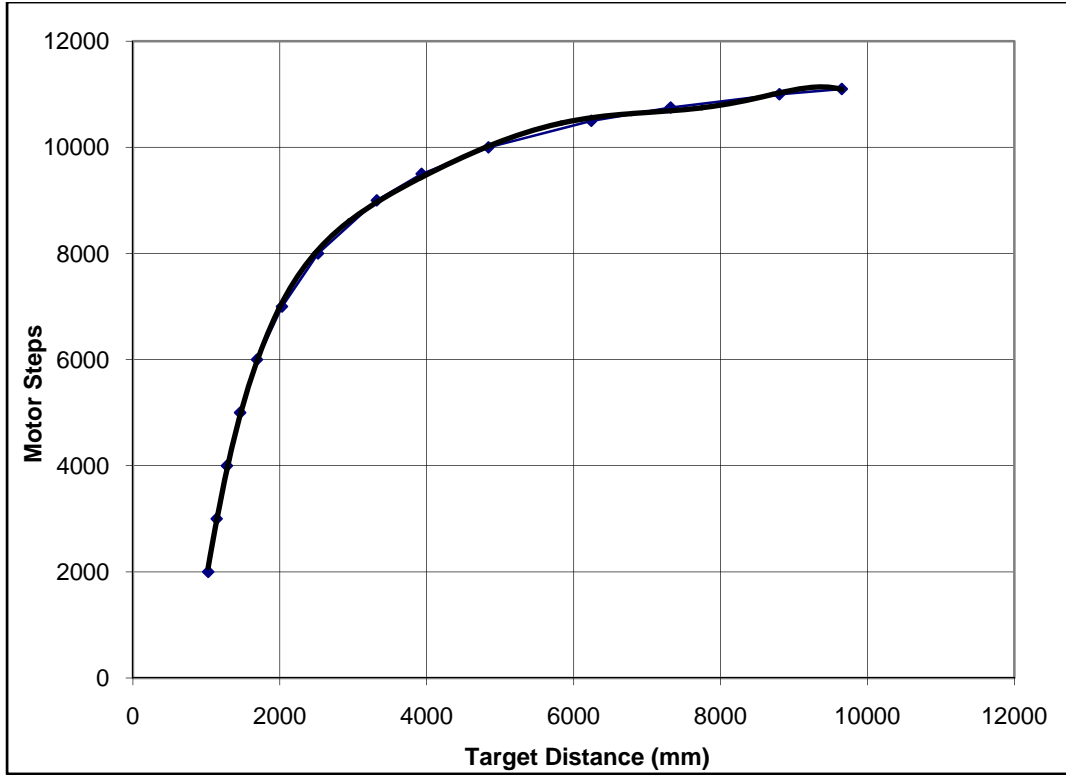


Figure 5 – Motor Steps versus Target Distance Using Data Developed by the French Team

The data is fitted, in a least squares sense, to a polynomial equation using MATLAB's curve fitting toolbox as follows:

$$m_s = 9006 \exp(2.281E - 05d) - 2.2146E04 \exp(-1.082E - 03d) \quad (2)$$

where m_s is the number of motor steps and d is the target distance. The mast cameras on the rover provide the target distance to $\pm 5\%$. Inputting the target distance (mm), d , obtained from the mast cameras into the above equation will determine the number of motor steps to achieve the approximate laser focus distance. However, since this distance is accurate to only $\pm 5\%$, a method will be selected that focuses the LIBS laser to a much finer resolution, one that is suitable to focus the laser to a small enough focal point at target to produce the desired plasma.

Similarly, the target distance versus motor step is also equated; a formula that would be used if a value for motor steps was known and a target distance was needed:

$$d = 8.077E - 03 \exp (1.212E - 03m_s) + 682 \exp (1.577E - 04m_s) \quad (3)$$

During experimentation described in the next chapter, a motor step increment of 50 was visually observed to create plasma at a sufficient number of laser shots (7 out of 12 shots) to ensure that a maximum amount of plasma light signal could be optimized at a target distance of 1.5 meters. However, as the target distance was increased, visual plasma observations in the lab showed that the motor step increment was necessarily decreased due to the relationship of motor steps. To simplify the calculations required by the onboard microprocessor, a linear relationship between motor turns and target distance was fitted (Figure 6).

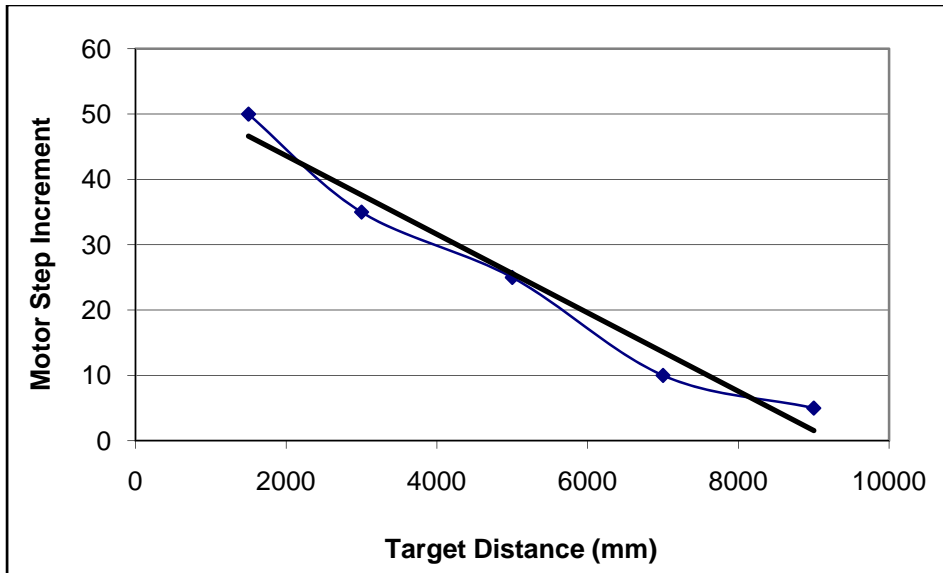


Figure 6 – Motor Step Increment Determination Chart

The line fit for this data is as follows:

$$inc = -0.006d + 55 \quad (4)$$

where inc is the motor step increment and d is the target distance as before. When the rover reports a target distance, the motor step (2) and motor step increment (4) equations are used to search for a target plasma light signal. The plasma light signal will be present when plasma is generated at the target and that signal is distinguishable from the noise (ambient light).

Using Equations 2 and 4, Table 5 compiles the factors that influence target shots. Column 1 contains some representative target distances and Column 2 is computed using Equation 4. Columns 3, 4 and 5 are 95%, 105% and 10% of Column 1. Columns 6, 7 and 8 are computed using Equation 2. Number of Shots on Target (Column 9) is calculated by dividing the delta Motor Steps (column 8) by the Motor Step Increment (Column 2). However, when the Number of Shots on Target is less than ten, the value will be increased to ten to ensure that enough laser shots are fired to find the maximum signal. This means that distances of 2500 \rightarrow 7500 mm will be increased to ten laser shots.

Table 5 - Laser Focusing Statistics

Target Distance (mm)	Motor Step Increment	95% of Target Distance (mm)	105% of Target Distance (mm)	delta (105-95)% (mm)	Motor Steps at 95% of TD	Motor Steps at 105% of TD	delta Motor Steps	No of Shots on Target
1500	50	1425	1575	150	4755	5485	730	15
2000	47	1900	2100	200	6690	7233	544	12
2500	44	2375	2625	250	7804	8195	391	9
3000	41	2850	3150	300	8475	8777	302	7
3500	38	3325	3675	350	8929	9200	271	7
4000	35	3800	4200	400	9289	9559	270	8
4500	32	4275	4725	450	9607	9876	269	8
5000	29	4750	5250	500	9890	10137	248	9
5500	26	5225	5775	550	10126	10326	200	8
6000	23	5700	6300	600	10304	10439	135	6
6500	20	6175	6825	650	10418	10494	76	4
7000	17	6650	7350	700	10480	10532	52	3
7500	14	7125	7875	750	10515	10597	83	6
8000	11	7600	8400	800	10557	10721	164	15
8500	8	8075	8925	850	10637	10880	243	30
9000	5	8550	9450	900	10765	10959	194	39

Chapter 2 - Focusing Methods

The focusing methods considered include:

Method 1 – Hunt Through Entire Range

Incrementing the secondary mirror position, fire the LIBS laser at each increment through the entire target distance range of the instrument ($1.5 \rightarrow 9$ meters); optimizing a cost function described by the spectral data (Appendix C).

Method 2 – Hunt Through Camera Determined Distance Range of $d \pm 0.05d$

Using the camera-determined distance, increment the secondary mirror position, fire the LIBS laser at each increment through the camera distance error range of $d \pm 0.05d$; optimizing a cost function described by this range of spectral data (Appendix B).

Method 3 – Hunt Partially Through Camera Determined Distance Range

Using the camera-determined distance, increment the secondary mirror position; fire the LIBS laser at each increment while optimizing a cost function to stop right after the maximum detection of signal.

To find a maximum amount of plasma light signal present, each of the three methods described above requires the development of a cost function [4] particular to the method selected. Also, baseline, reference spectra of the background light is captured, processed and stored. Thresholds above the baseline are calculated from the background data in the form of standard deviations that are determined by the data.

Prior to implementing the algorithm, the time duration of firing the laser will be quantified and the algorithm will be optimized to minimize total time. A potential optimization technique is to fire the laser at 95% and 105%, bisect these values and

continue bisecting until plasma is indicated. Upon the detection of plasma, the algorithm would then narrow in on the maximum by applying a Golden Section Search as described in Chapter 5.

Method 1, described above, requires the most laser shots (~225), data processing/storage and time to complete of the three methods. This method is estimated to take 2 hours to execute at one minute per laser shot. Method 1 would have the most variability in the background noise (ambient light) since the Martian day (sol) will progress as the method is being executed. The change in angle of the sun would increase or decrease the background noise, which would affect the baseline established for the method. This phenomenon may render Method 1 ineffective, except at night.

Method 2 would require far fewer laser shots (between 10 and 40) than Method 1. The time required to execute Method 2 would be between 10 and 40 minutes, depending on the distance to target. There would be less background noise fluctuation because of the shorter time to perform the method.

Method 3 is similar to Method 2 except that laser shots would cease right after the peak of the cost function is detected. This method would require the least amount of time (5 - 20 minutes), the least amount of data processing and would have the least amount of background noise fluctuation. Method 3 would stop right after the cost function is maximized.

The focusing methods chosen are Methods 1 and 2. Method 1 finds the laser focus distance at night while Method 2 finds the maximum signal with the least chance of making an error due to false maximums.

The flowchart in Figure 7 provides the logic:

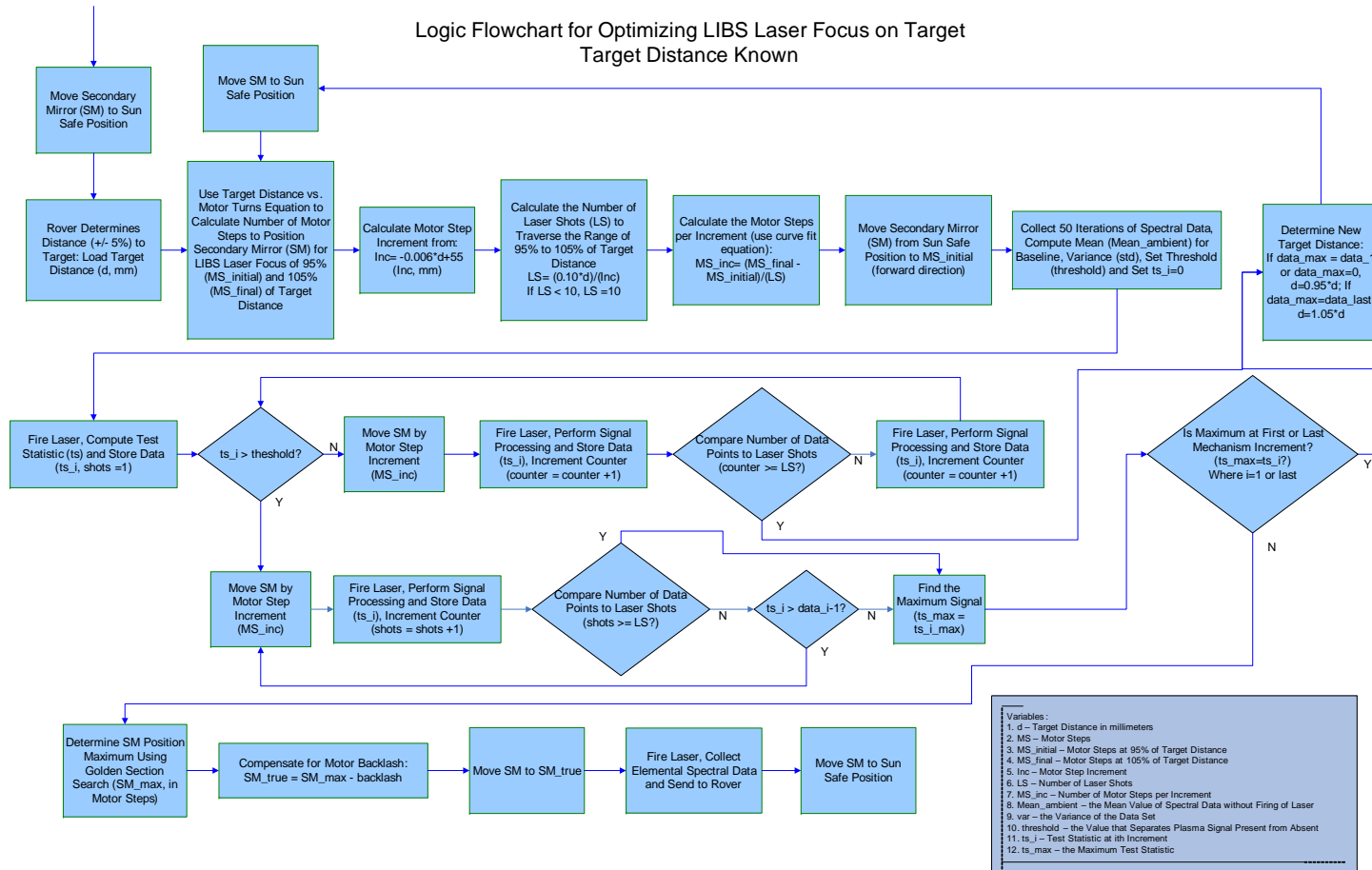


Figure 7 - Logic Flowchart for Focusing and Optimizing the LIBS Laser on Target, Target Distance Known

Chapter 3 - Engineering Model Experiments, Data and Analysis

The implementation of the methods of Chapter 2 requires the performance of experiments on the actual hardware to assess the concept. This is accomplished using the Engineering Model (EM), a prototype ChemCam instrument installed at LANL to test and debug the hardware and software (Figure 8). The experiments will also be used to evaluate the strength of the light signal from the plasma for different target distances and to optimize the motor step increment amount to move the secondary mirror while searching for the optimum target distance.

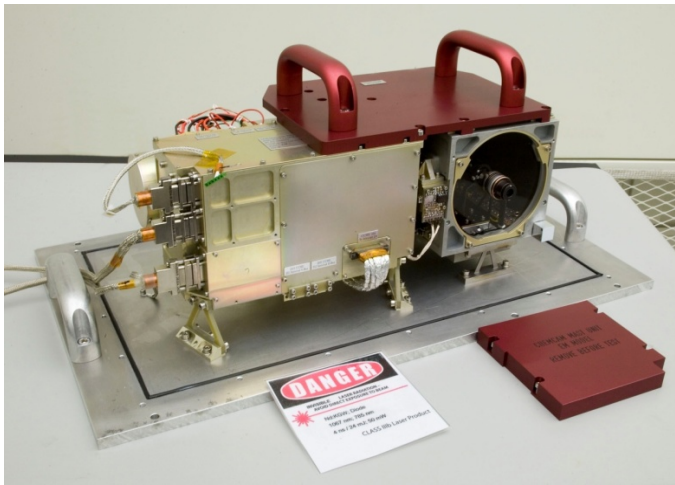


Figure 8 – Prototype ChemCam Instrument Mast Unit (Engineering Model)

Experiment Number 1

The first experiment was performed on consecutive days (October 11 & 12, 2007) in a laser lab at LANL with standard temperature and pressure. Note that the standard atmospheric pressure in Los Alamos is 0.76 atm because the elevation is 2,200 m. The background light in the lab is fluorescent and the temperature is controlled at 20°C. The target used is an Aluminum alloy plate mounted on a cart in the open air and the target distances selected are 1.5, 3.0, 5.0, 7.0 and 9.0 meters. The

LIBS laser was operated in single-pulse mode and the SM was actuated incrementally using computer commands.

The target was placed at distances of 1.5 and 5.0 meters on October 11 and at distances of 3.0, 5.0 and 7.0 meters on October 12. The cameras were not used; distances were measured with a measuring tape. At 1.5, 5.0 and 9.0-meter distances, the secondary mirror was moved to 95% of the measured target distance using the motor steps versus target distance equation (1) and incremented through the measured target range. The list of ChemCam instrument computer commands necessary to complete the experiments can be found in Appendix A.

Laser shots were fired according to Table 6. Column 1 is the distance as measured while column 2 was computed using Equation 1. Column 3 contains the distances in which a laser shot was fired and Column 4 is a visual qualitative indicator of the effect of the laser on the target. Column 5 is the data file identifier.

The qualitative observations in Column 4 are visual and auditory indications made by the experimenters. A tick means a sound was made without observing plasma light. A spark is a small amount of light and a plasma entry in the table means a larger amount of light at the target was observed. Figure 15's spectrographs illustrate that no observable light content on the 4th shot and only small peaks on the 5th shot corresponding to the tick sound and spark recorded in the table.

Table 6 – Increment Experiment Data

Target Distance (mm, measured)	Number of Motor Steps	Target Distance (mm, calculated)	Visual Plasma Indication	Data File ID
1500	4928	1450	no plasma	144514
	4978	1455	no plasma	145732
	5028	1461	no plasma	150413
	5078	1467	tick sound	150849
	5128	1473	spark	151355
	5178	1479	plasma	151957
	5228	1486	plasma	152406
	5278	1493	plasma	153101
	5328	1500	plasma	153617
	5378	1508	spark	153955
	5428	1515	spark	154439
	5478	1524	weak tick	154655
3015	8648	3035	spark	210922
	8673	3054	spark	211042
	8698	3073	light spark	211143
5001	9519	3911	no plasma	160139
	9569	3982	no plasma	160536
	9619	4057	no plasma	160944
	9669	4135	no plasma	161153
	9969	4700	spark	163417
	10019	4813	spark	165332
	10069	4932	plasma	163633
	10119	5058	plasma	163916
	10169	5190	tick	164205
6985	10655	6934	spark	204952
	10665	6981	spark	205113
	10675	7028	plasma	205237
	10685	7075	spark	205357
	10695	7123	spark	205528
	10705	7171	spark	205643
9020	11016	8963	spark	200643
	11026	9031	spark	200905
	11031	9065	spark	201211
	11036	9099	spark	201351
	11041	9134	spark	201531
	11046	9168	spark	201651
	11051	9203	spark	201809
	11056	9238	spark	201928
	11061	9273	light spark	202045
	11066	9309	light spark	202303

The next plots show composites of all the data files detailed in Table 6 with the infrared, visible and ultraviolet spectrums plotted separately:

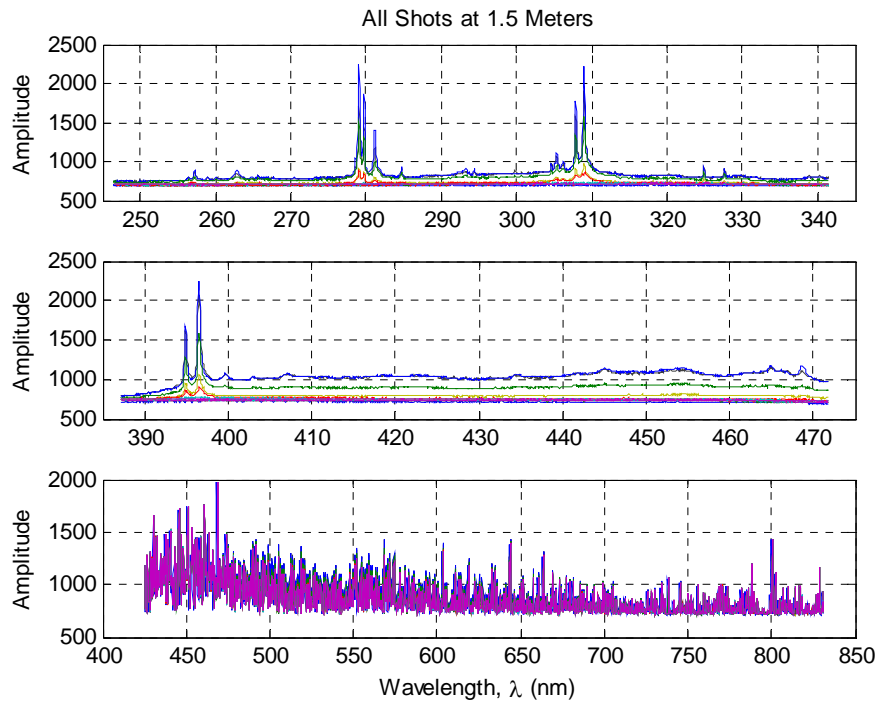


Figure 9 – Spectra Composite of 12 Laser Shots at 1.5 m Target Distance

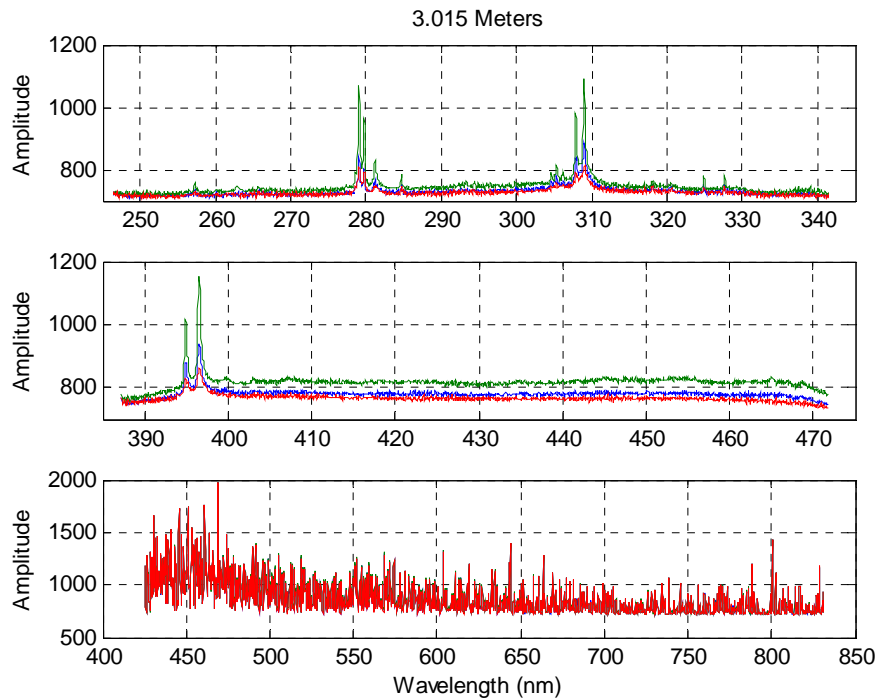


Figure 10 – Spectra Composite of 3 Laser Shots at 3 m Target Distance

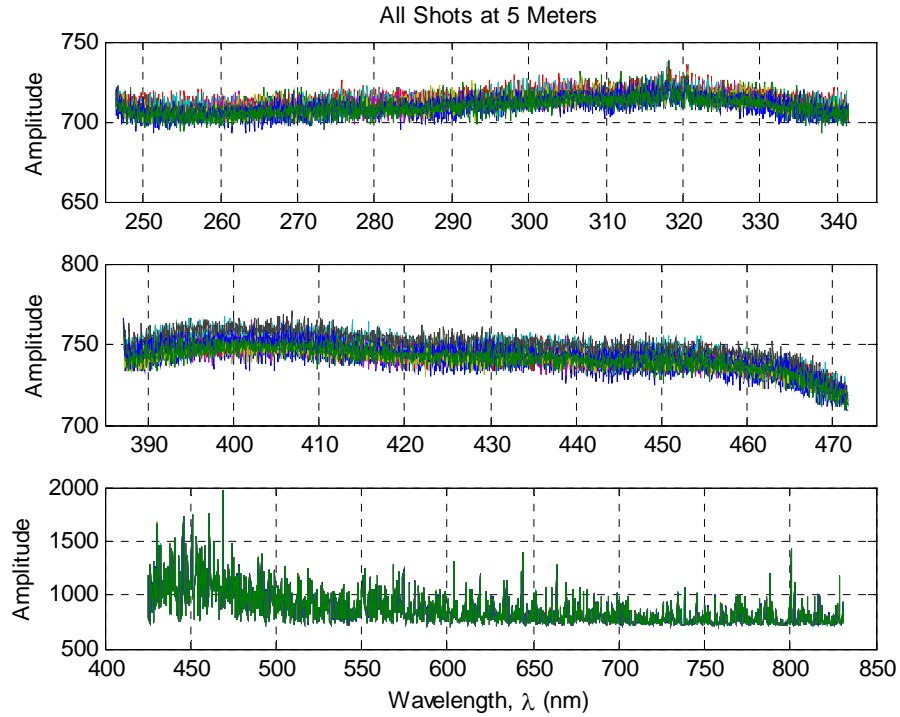


Figure 11 – Spectra Composite of 9 Laser Shots at 5 m Target Distance

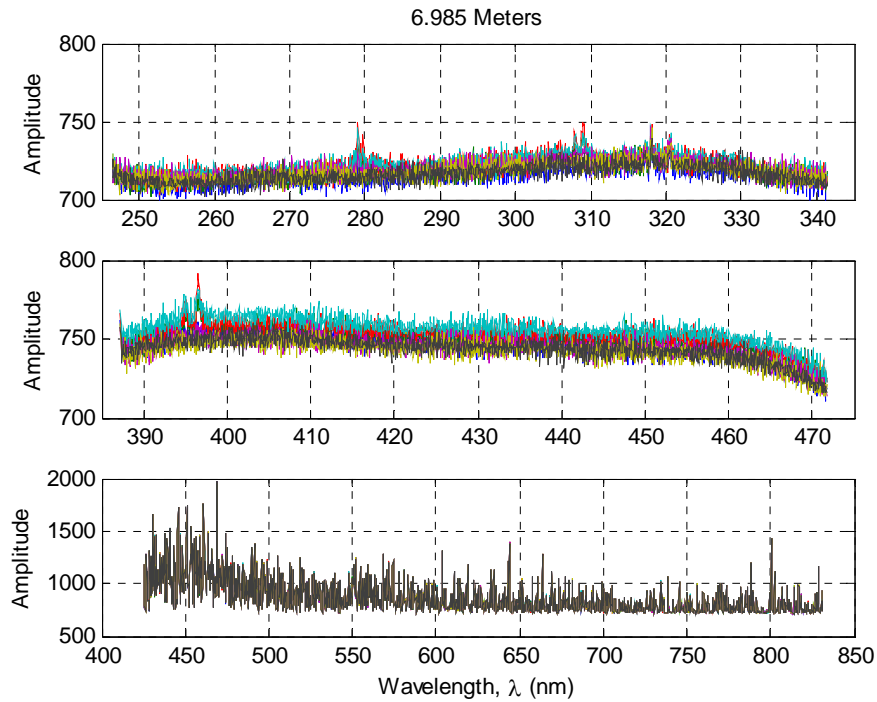


Figure 12 – Spectra Composite of 6 Laser Shots at 7 m Target Distance

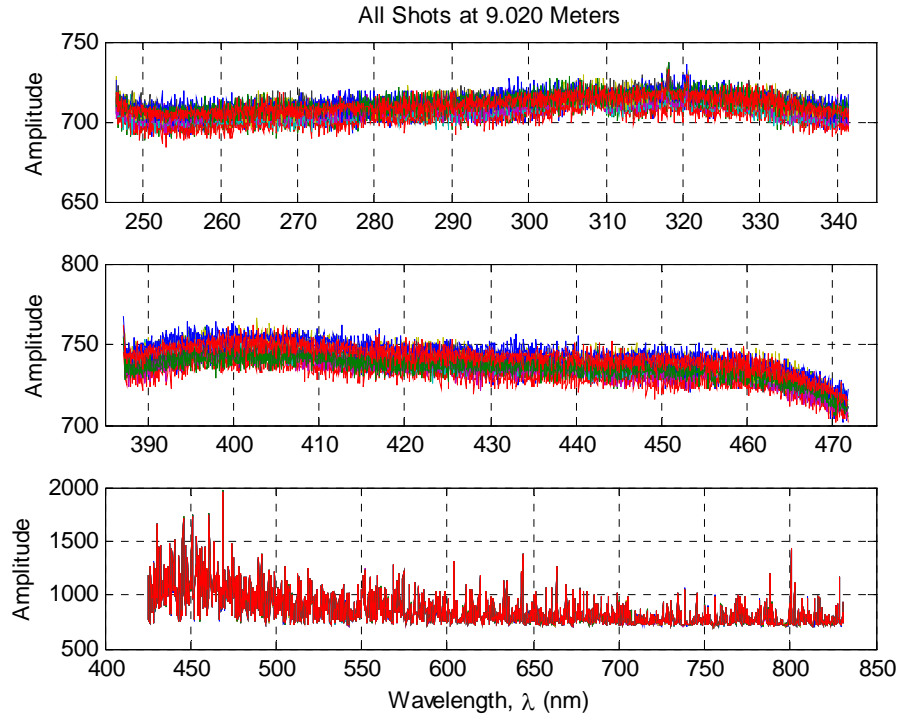


Figure 13 – Spectra Composite of 10 Laser Shots at 9 m Target Distance

In Figures 9 through 13, the spectral peaks are more prominent at the closer target distances and mostly obscured by noise beyond 3 meters. The ultraviolet and visible spectrometers at 1.5 and 3.0 meters show amplitude offset for all wavelengths that increases as the spectral peaks increase. This phenomenon is an important feature that is exploited in the development of the detector in Chapter 4 and is due to the thermal effects produced by the plasma and is not spectral leakage.

Clearly, the noise is a substantial component of the signal beyond 3 meters. Also, the very near infrared (vnir, 413→839 nm) spectrometer has an issue that would be resolved later in the instrument development so is not used, at this point, to formulate any conclusions in the project.

The next plots show the data broken out individually from Figure 9, obtained by incrementing the secondary mirror through the target distance of 1.5 m. A total of twelve

laser shots were fired at increments of 50 motor steps. Figures 14 through 17 show the ultraviolet spectra and Figures 18 through 21 shows the visible spectra in sequential order. Only the ultraviolet and visible spectra are plotted because the infrared spectrometer was malfunctioning during the experiment. Of the twelve laser shots, shots five through eleven created a plasma or spark by the experiment team's visual observations in the lab. The strongest plasma occurred at shot number eight and is shown separately in Figures 22 and 23.

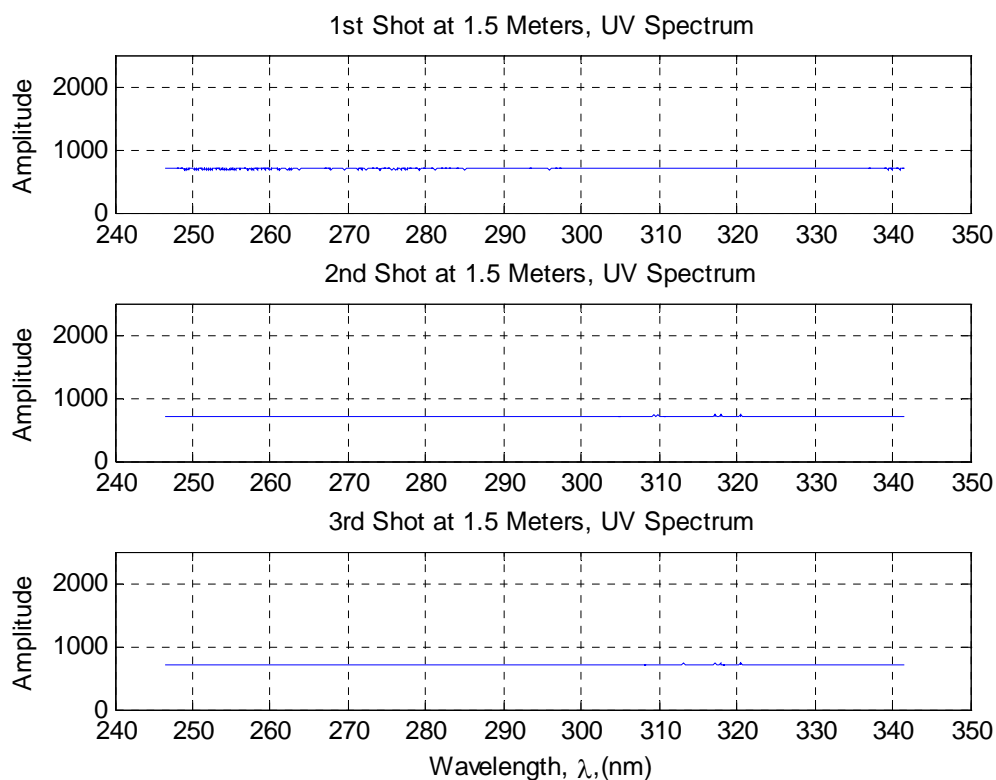


Figure 14 – Ultraviolet Light Spectra at 1.5 Meters, Shots 1 through 3

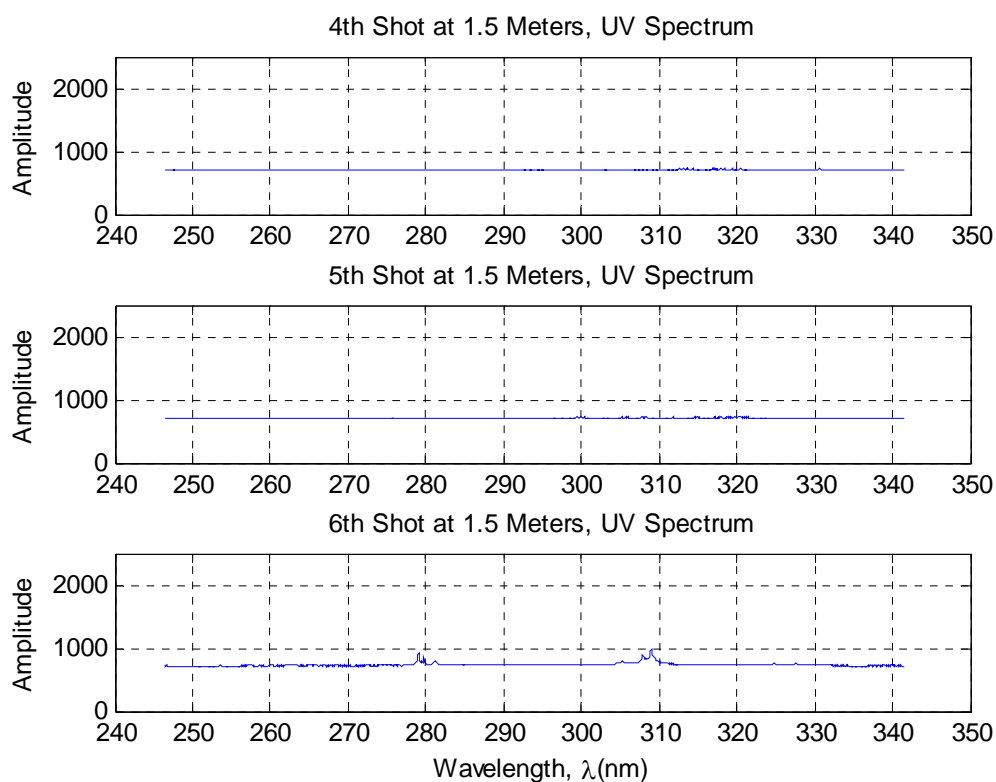


Figure 15 – Ultraviolet Light Spectra at 1.5 Meters, Shots 4 through 6

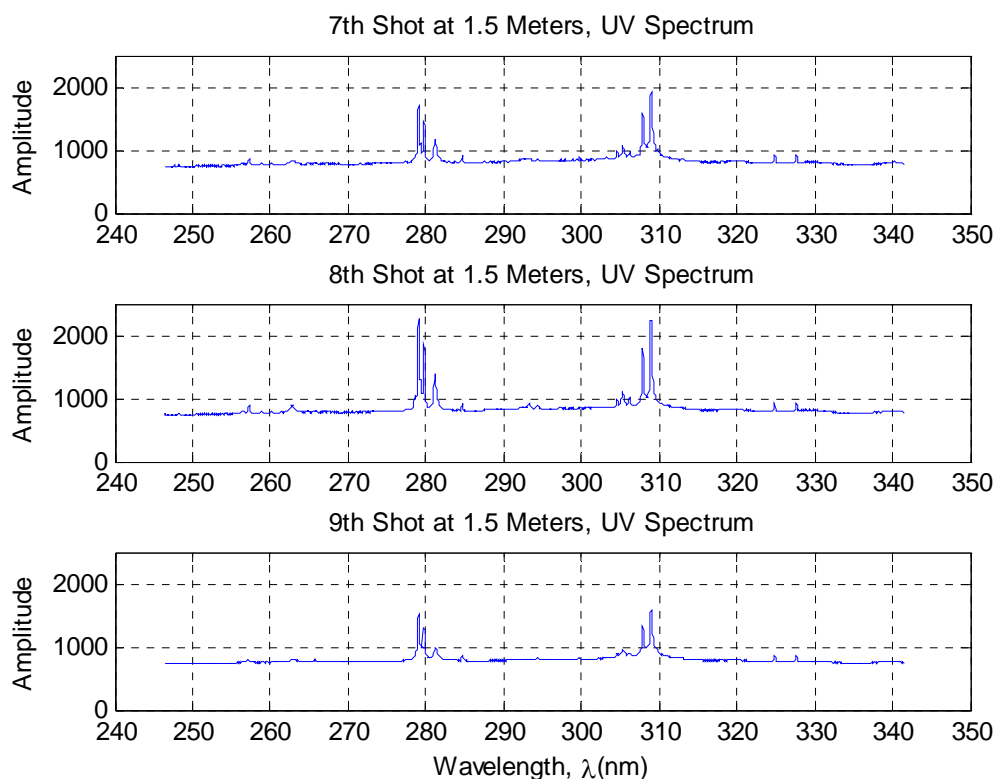


Figure 16 – Ultraviolet Light Spectra at 1.5 Meters, Shots 7 through 9

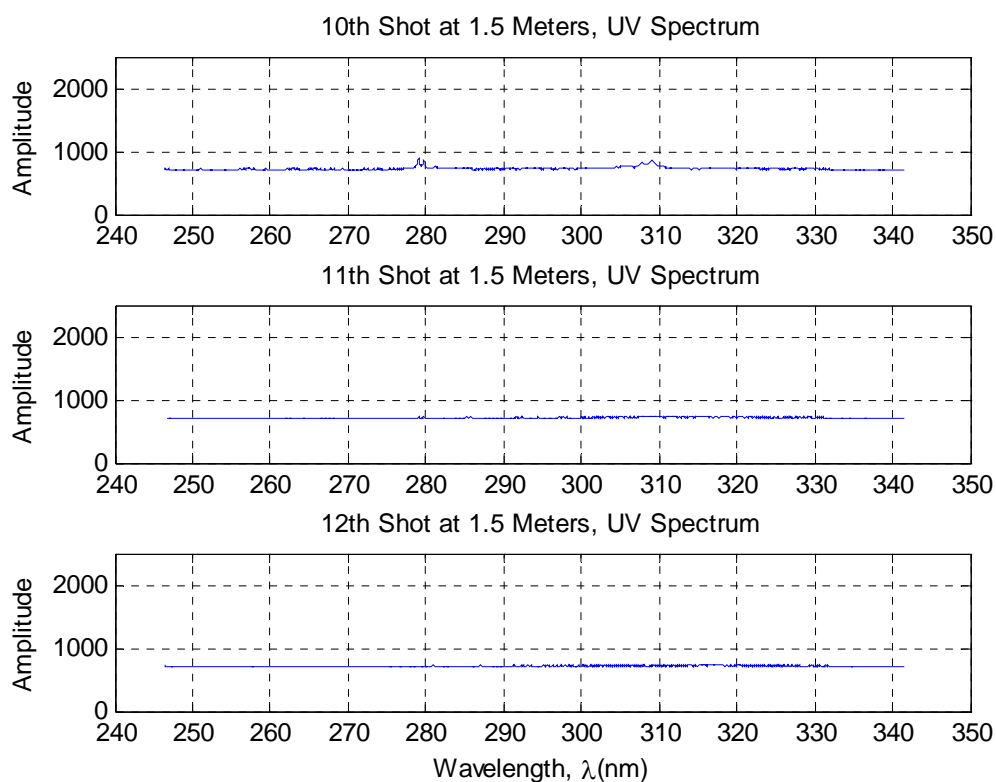


Figure 17 – Ultraviolet Light Spectra at 1.5 Meters, Shots 10 through 12

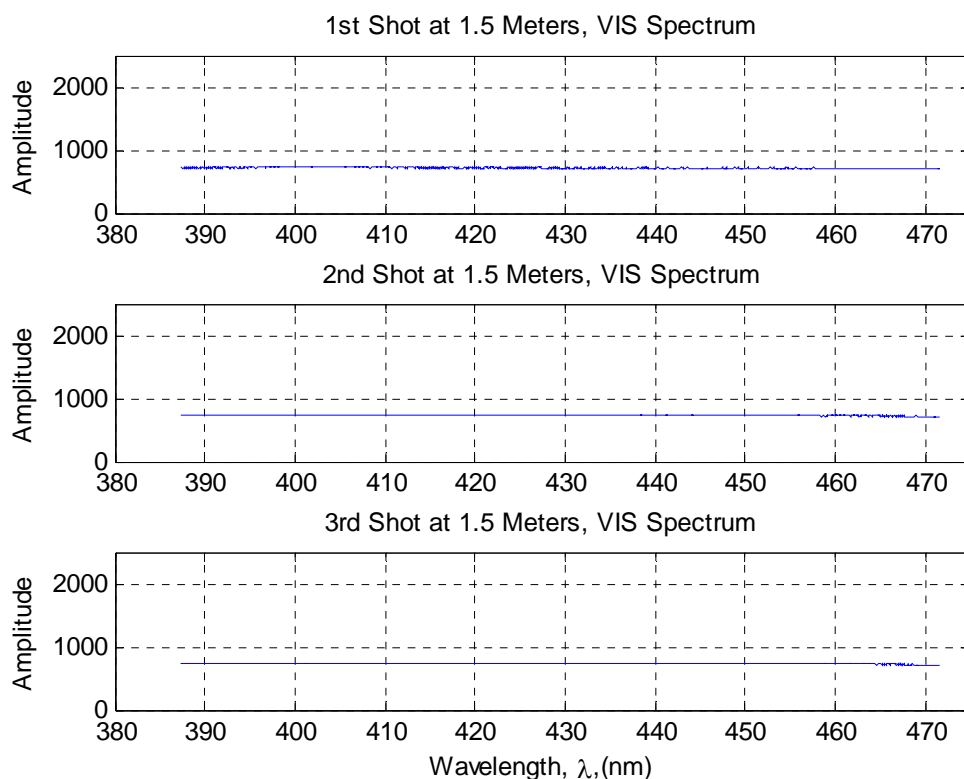


Figure 18 – Visible Light Spectra at 1.5 Meters, Shots 1 through 3

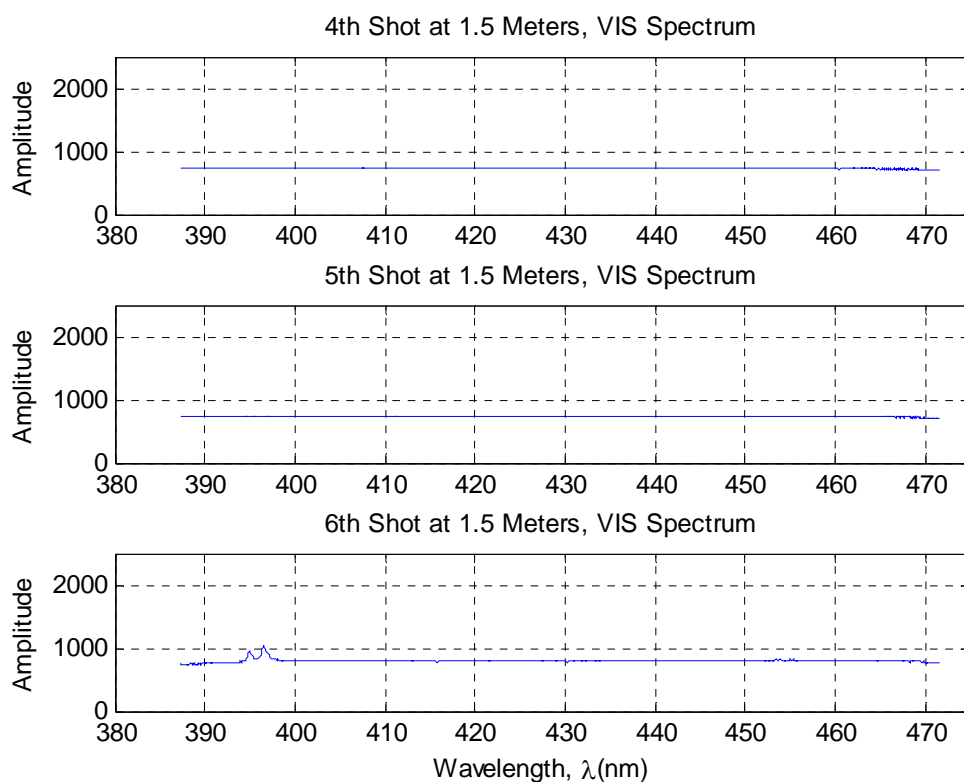


Figure 19 – Visible Light Spectra at 1.5 Meters, Shots 4 through 6

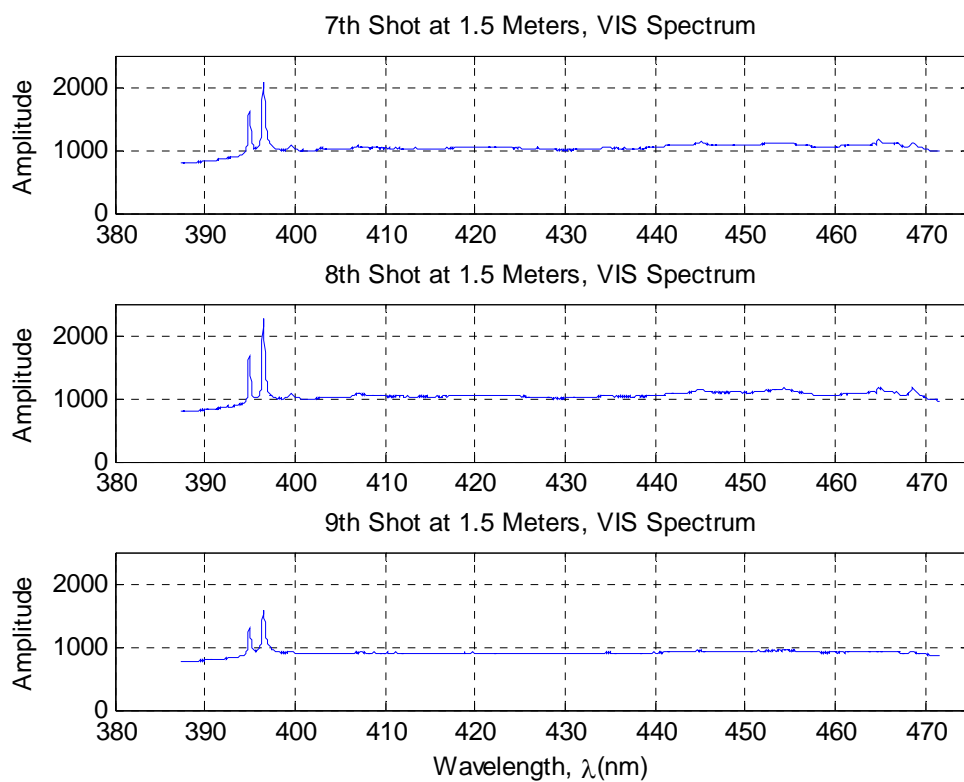


Figure 20 – Visible Light Spectra at 1.5 Meters, Shots 7 through 9

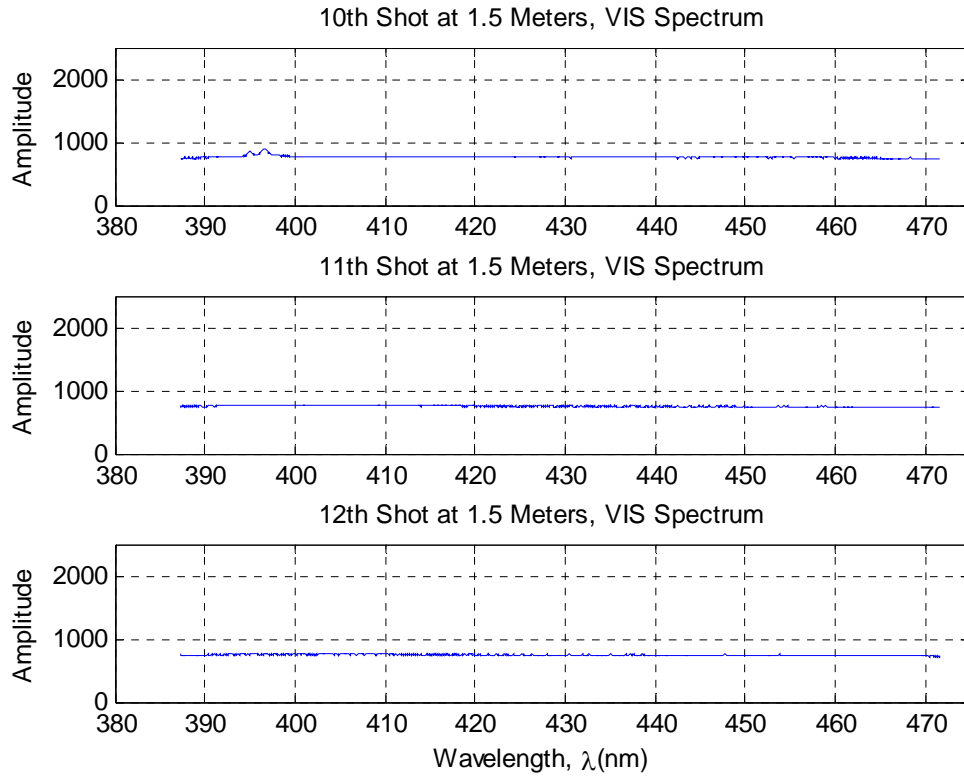


Figure 21 – Visible Light Spectra at 1.5 Meters, Shots 10 through 12

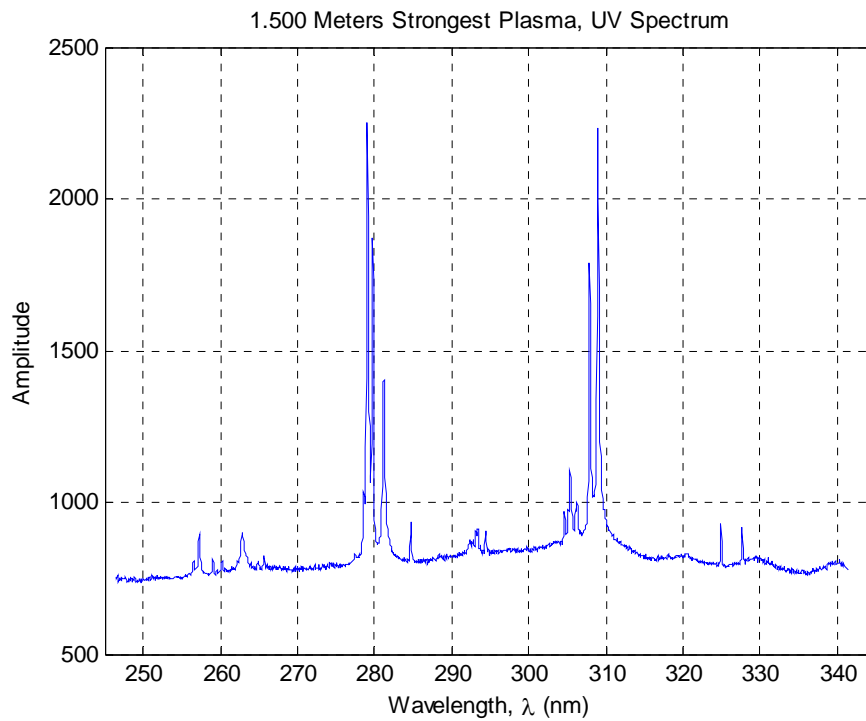


Figure 22 – Ultraviolet Light Spectrum at 1.5 Meters (8th Shot)

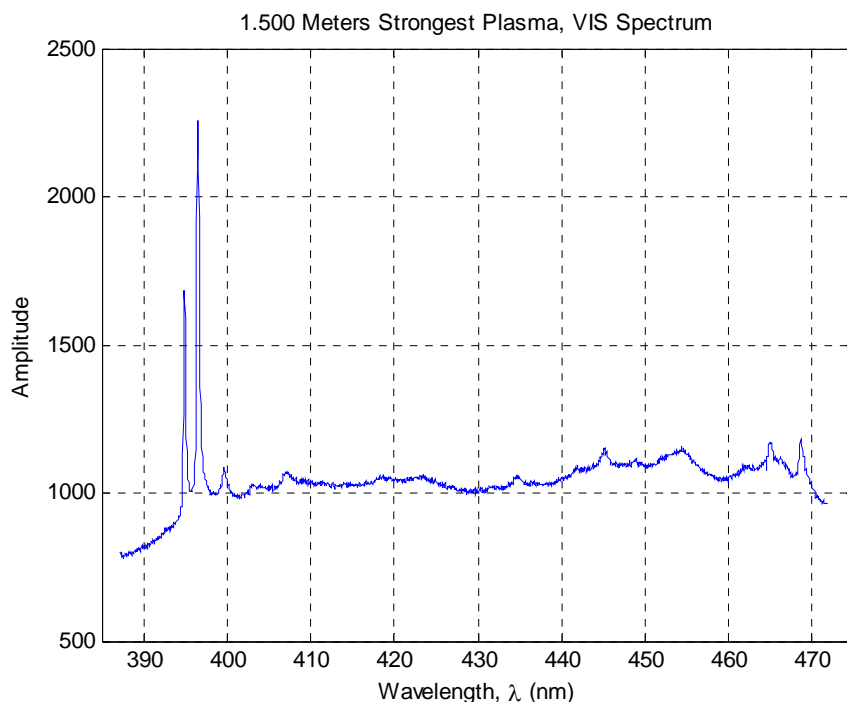


Figure 23 – Visible Light Spectrum at 1.5 Meters (8th Shot)

Based on these plots, the method of incrementing the secondary mirror through the target distance will produce signal data that can be differentiated from pure noise. The pure noise is represented by relatively flat lines across the wavelengths of the spectrometers and signal data has amplitude offset and prominent peaks at particular wavelengths associated with distinguishable elements.

When the peaks are not present in the spectral data, a “signal absent” hypothesis is postulated and the data set will represent noise without signal.

The next plots, Figures 24 through 26 show the same progression for the 9 meter target distance. Note the dominance of the plots by noise, it is difficult, if not impossible to detect a signal in this data. The visual observation in the lab indicated that the 3rd shot was the strongest spark but, as can be seen, this plot is not different from the others. However, the expectation by the project team is that the instrument performance will improve substantially when operating at the design conditions on Mars especially when

exposed to the Martian temperatures. Therefore, the development of the methods for this project will assume that a distinguishable signal can be statistically delineated from the noise within the full target range of the instrument but the actual data will determine the limits.

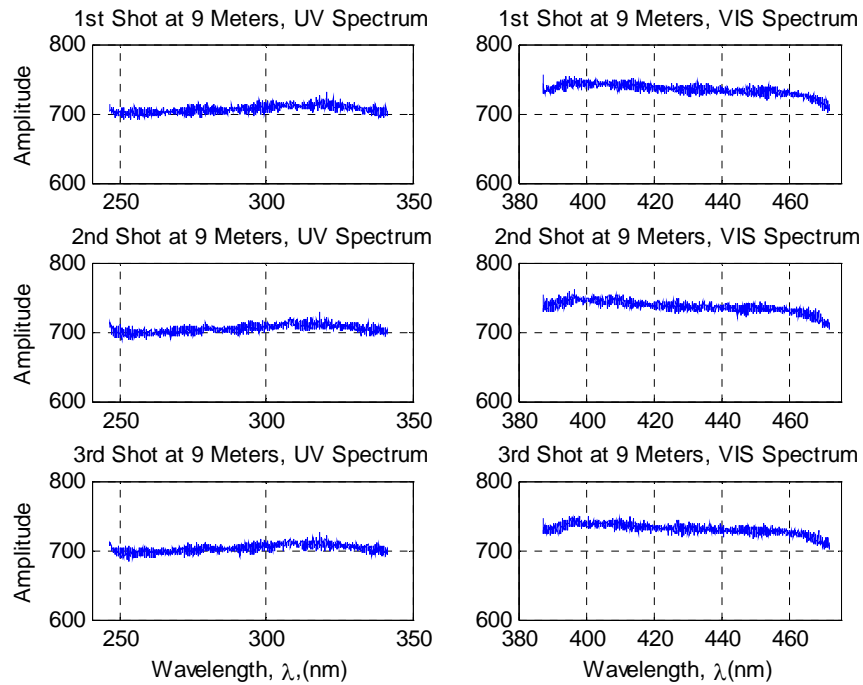


Figure 24 – Ultraviolet and Visible Light Spectra at 9 Meters (1st through 3rd Shots)

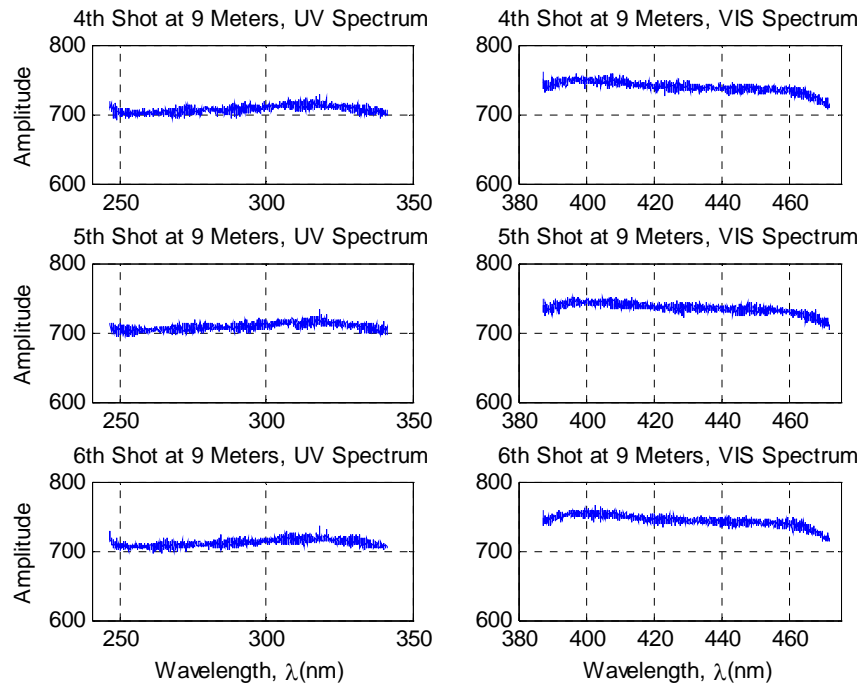


Figure 25 – Ultraviolet and Visible Light Spectra at 9 Meters (4th through 6th Shots)

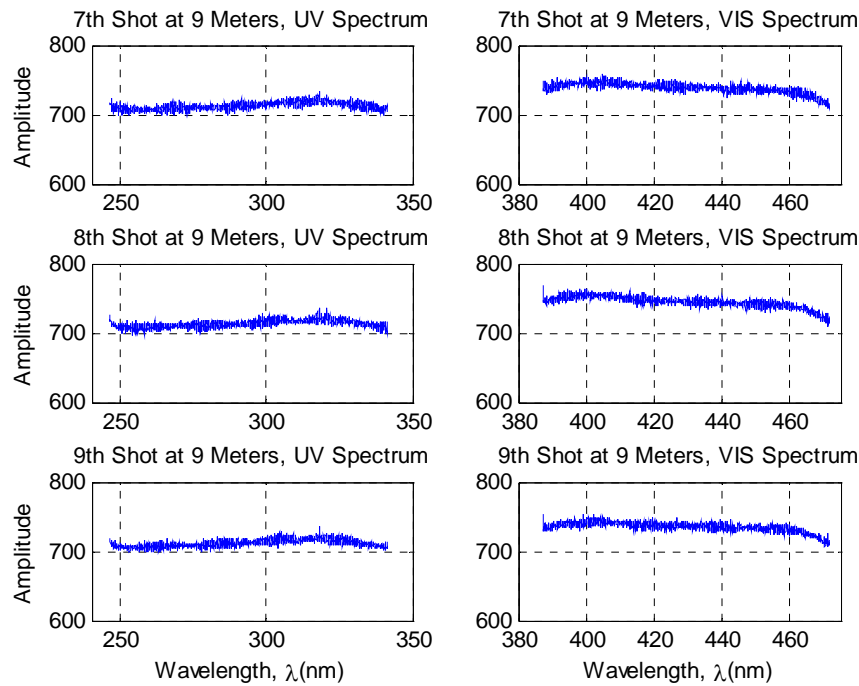


Figure 26 – Ultraviolet and Visible Light Spectra at 9 Meters (7th through 9th Shots)

In Experiment 1, the target plate was made of black anodized, 6061 Aluminum; the chemical composition is shown in Table 8. The oxygen contained in the anodized surface was not detectable in the plasma spectra:

Table 7 – Chemical Composition of Aluminum 6061

Component	Amount (wt.%)
Aluminum	Balance
Magnesium	0.8-1.2
Silicon	0.4 – 0.8
Iron	Max. 0.7
Copper	0.15-0.40
Zinc	Max. 0.25
Titanium	Max. 0.15
Manganese	Max. 0.15
Chromium	0.04-0.35
Others	0.05

Table 9 shows the spectral lines for the principal elements in Table 8:

Table 8 – Main Lines in Atomic Spectrum of Aluminum 6061 [6]

Aluminum	Magnesium	Silicon	Copper	Chromium
308.215 nm	279.533 nm	251.611 nm	216.509 nm	357.869 nm
309.271 nm	280.270 nm	288.156 nm	217.894 nm	359.349 nm
309.281 nm	285.213 nm	504.103 nm	324.754 nm	360.533 nm
394.401 nm	383.829 nm	505.598 nm	327.396 nm	425.435 nm
396.152 nm	518.361 nm	566.956 nm	521.820 nm	427.480 nm
		634.710 nm		428.972 nm
		637.136 nm		520.844 nm

Referring to Figure 22 and 23, peaks at the wavelengths for Aluminum are clearly seen. Three of the wavelengths for Magnesium have peaks in Figure 22: 279.533, 280.270 and 285.213 nm. Copper can be distinguished in Figure 22 at wavelengths of 324.754 and 327.396 nm. The magnitude of the Magnesium spectral lines was totally unexpected since this element only makes up 0.8 – 1.2% of the alloy. Also, the detection of Copper at 0.15 – 0.40% was also not expected. These data show that the elemental

detection of LIBS is robust. However, the amount of energy produced in the plasma by the individual elements does not scale with the concentration at the experimental conditions described. This phenomenon is due to the different amounts of energy released from the atom as the electrons jump to lower energy shells.

Experiment Number 2

The second experiment was performed on January 18, 2008 using the same hardware as Experiment 1 except the targets were placed in a vacuum chamber on a cart held constant at a 2 meter target distance and maintained at 7 Torr pressure. The targets were standard material samples depicted in Table 10.

Table 9 - Samples Used for Experiment 2 [7]

Sample #	Material	Composition
1	Dolomite	CaO, MgO
2	Dolomite	CaO, MgO
3	Dolomite	CaO, MgO
4	Gypsum	SO₃, CaO
5	Basalt	SiO₂, Al₂O₃, FeO, Fe₂O₃
6	Andesite	SiO₂, Si
7	Basalt	SiO₂, Al₂O₃, FeO, Fe₂O₃
8	Basalt	SiO₂, Al₂O₃, FeO, Fe₂O₃
9	Basalt	SiO₂, Al₂O₃, FeO, Fe₂O₃

In Experiment 2, 50 sets of background data were captured before firing the laser at each sample. Also, 50 sets of data were taken while firing the laser by pulsing it at 10 Hertz, 50 times. Figures 27 through 34 are averages of the 50 sets of data. The 50 sets of data are used in Chapter 4 to develop signal processing methods. Figures 27 through 34 show the averages of the 50 shots of background preceding the firing of the laser and the averages of the 50 shots of data while firing the laser for each spectrum of samples 1, 4, 7 and 9. Note that the averages are computed at each wavelength bin.

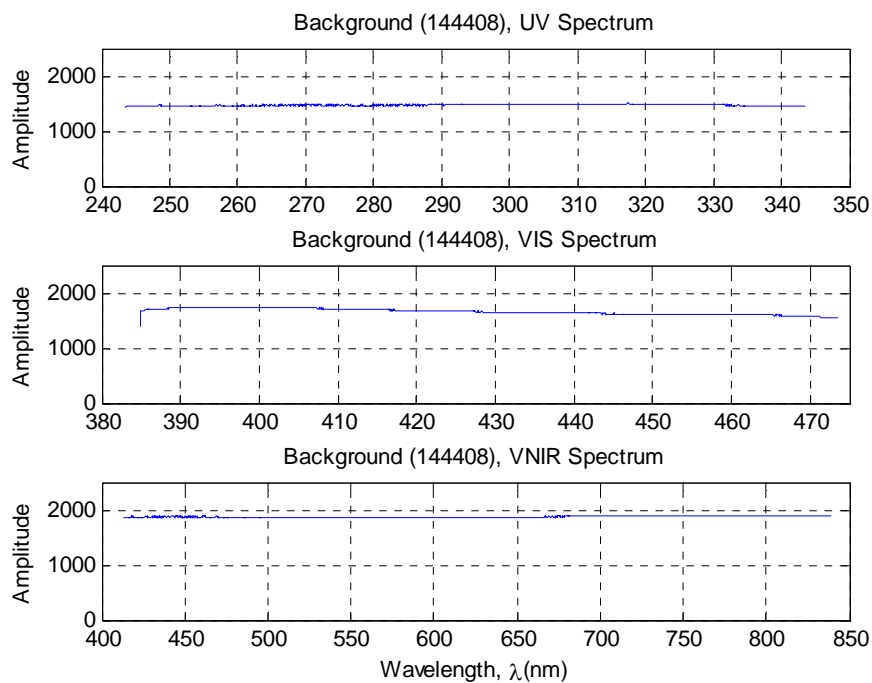


Figure 27 – Background Number 1 at 2m

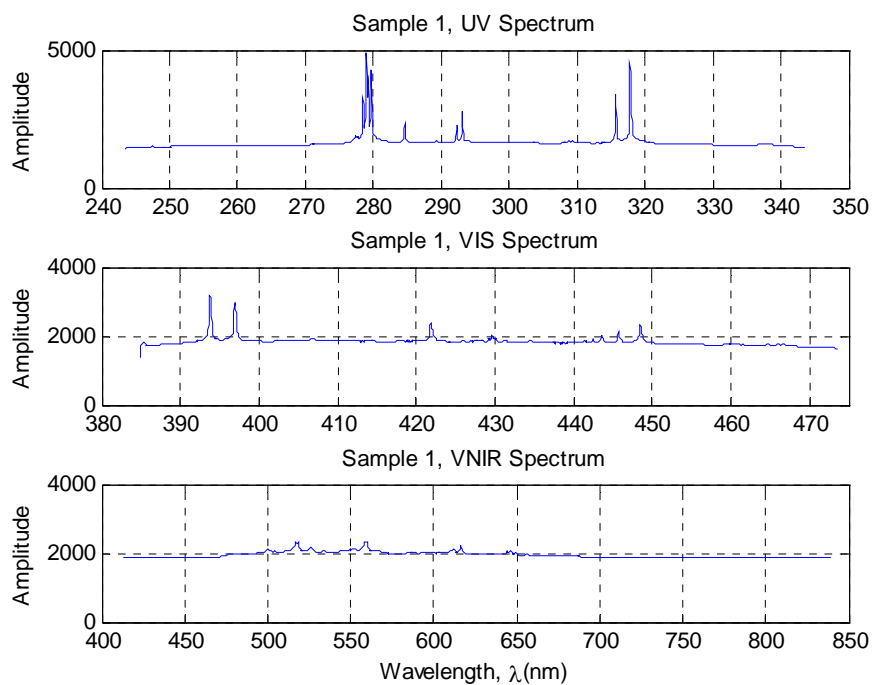


Figure 28 – Sample Number 1 at 2m

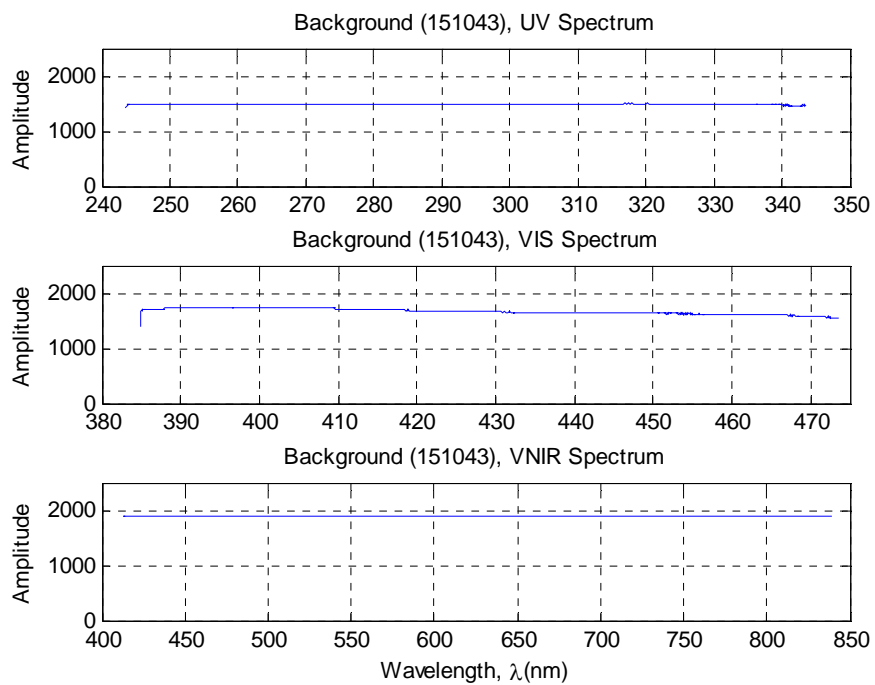


Figure 29 – Background Number 4 at 2m

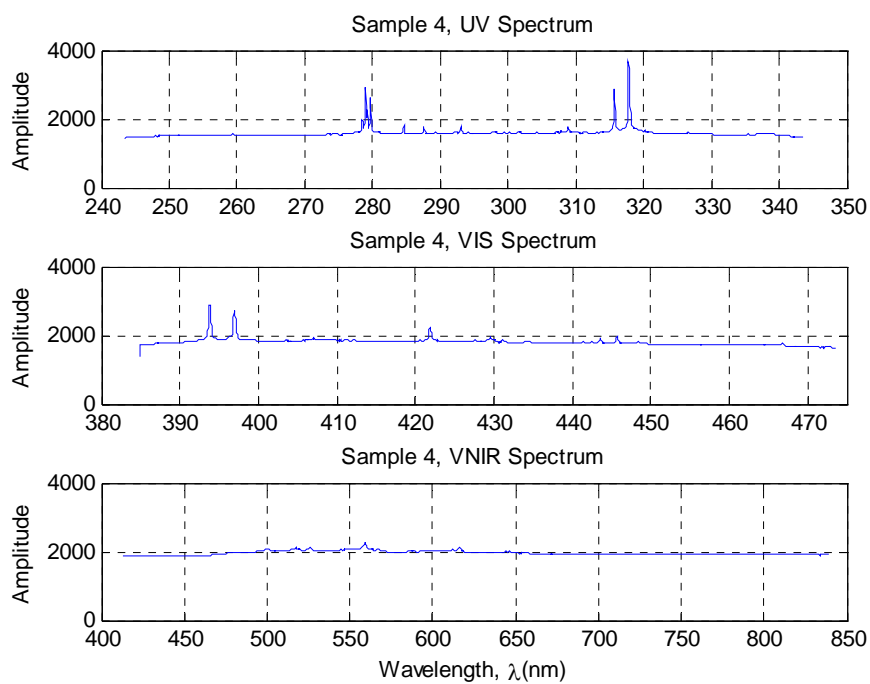


Figure 30 – Sample Number 4 at 2m

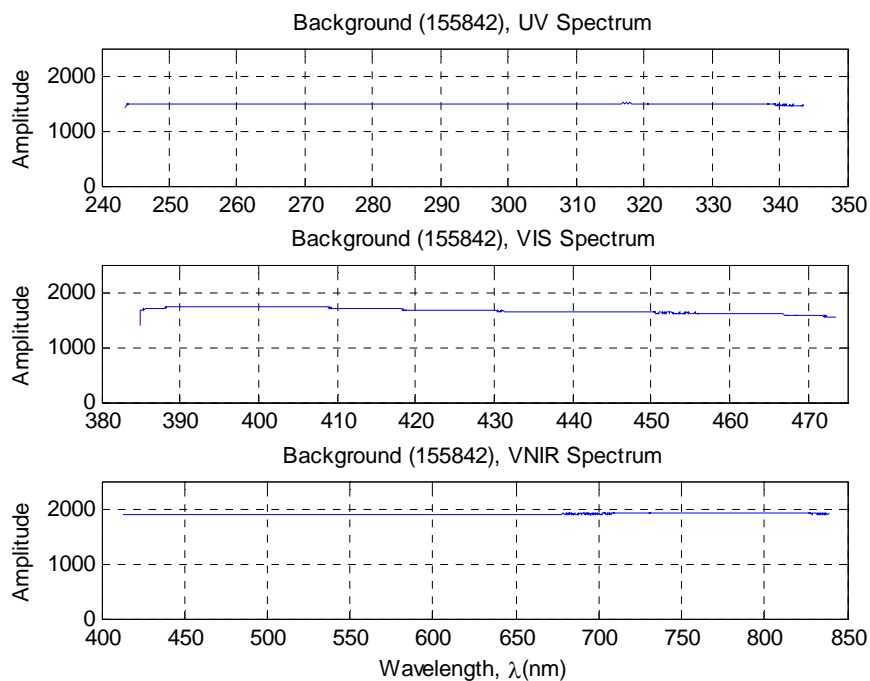


Figure 31 – Background Number 7 at 2m

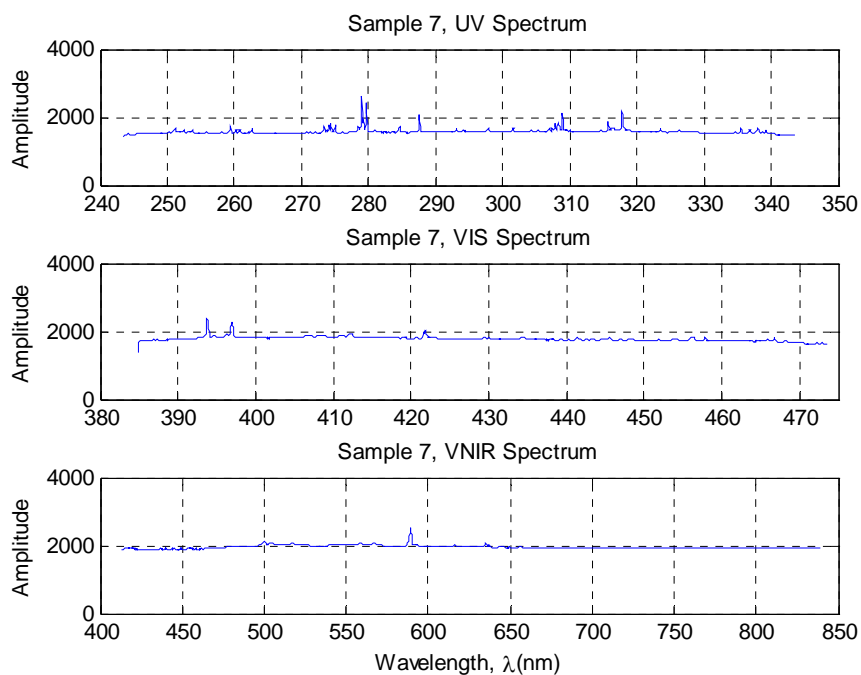


Figure 32 – Sample Number 7 at 2m

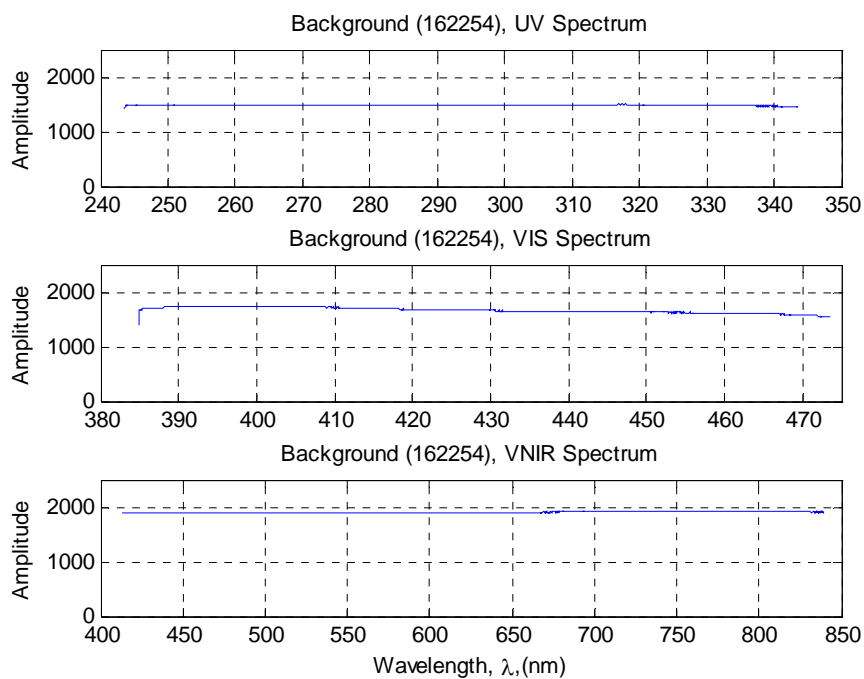


Figure 33 – Background Number 9 at 2m

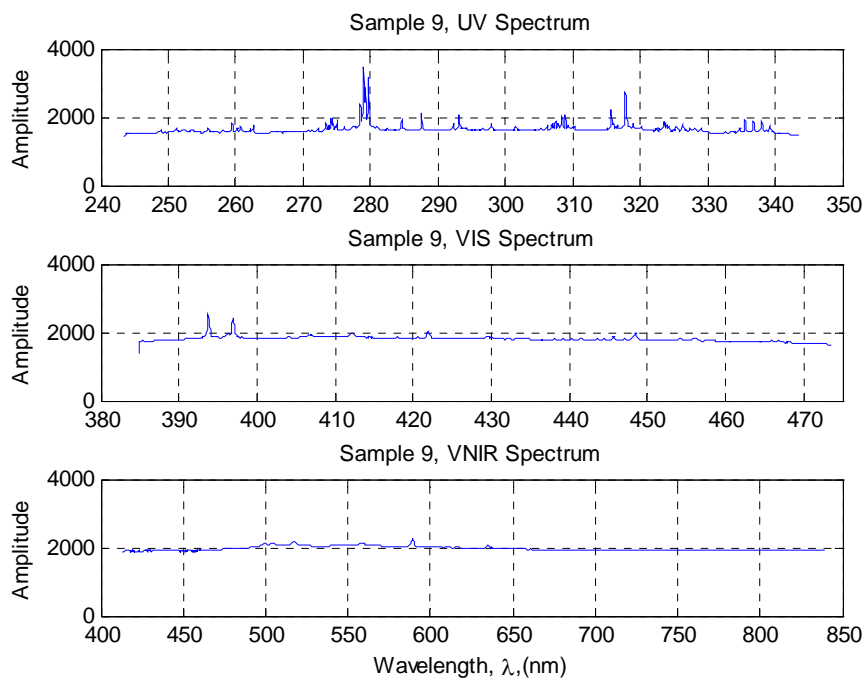


Figure 34 – Sample Number 9 at 2m

Chapter 4 - Signal Processing and Optimization

The hypothesis testing described in the Introduction and illustrated in Table 4, initiates the signal detection schemes that will now be developed [8]. This approach is a binary hypothesis test because it is a choice between two competing hypotheses: \mathcal{H}_0 and \mathcal{H}_1 . \mathcal{H}_0 is the null hypothesis (noise only) and \mathcal{H}_1 is the alternative hypothesis (signal plus noise):

$$\mathcal{H}_0: x[n] = w[n]$$

$$\mathcal{H}_1: x[n] = s[n] + w[n]$$

where $x[n]$ is the spectrometer data set, $w[n]$ is the background noise, $s[n]$ is the signal and n represents a wavelength index for the data.

The previous figures show that the background noise spectra are offset from zero. To simplify the test statistics, the background noise is transformed into zero mean, by subtracting the mean of the background data set from each data point and using the resulting data as the operational set (see Figure 35). The reduced background data set is calculated as follows:

$$x_r[n] = x[n] - \mu_r \quad (5)$$

where $x_r[n]$ are reduced data, $x[n]$ is $w[n]$ and μ_r is defined as follows:

$$\mu_r = \frac{1}{NM} \sum_{n=0}^{N-1} \sum_{m=0}^{M-1} x[n, m] \quad (6)$$

where μ_r is the mean of all background noise values obtained for each spectrometer, M is the number of data sets, N is 2048 for each spectrometer and $x[n, m]$ is the data obtained by taking background noise samples. In Experiment 2, x is 2048 rows by 50 columns for each spectrometer, which represents 50 data sets of 2048 wavelength bins. The mean

value is computed by evaluating Equation 6. The reduced noise is computed by subtracting the mean from each $x[n, m]$. These parameters are used in the first signal processing option, white noise, described below.

When the noise is colored, a second set of parameters are used to perform the signal processing:

$$x_r[n] = x[n] - \mu_r[n] \quad (7)$$

where $x_r[n]$ are the reduced noise samples, $x[n]$ is $w[n]$ and $\mu_r[n]$ is defined as follows:

$$\mu_r[n] = \frac{1}{M} \sum_{m=0}^{M-1} x[n, m] \quad (8)$$

where $\mu_r[n]$ is the mean of noise samples at each wavelength bin. This mean is computed by averaging the 50 shots of background at each wavelength bin captured in Experiment 2. The reduced noise, $x_r[n]$, is computed by subtracting the mean at each wavelength bin from each $x[n]$. These parameters are used in the second signal processing option, colored noise, described below.

The ChemCam instrument hunts for a plasma signal using the methods described in Chapter 2. The SM is positioned, the laser is fired and the data is captured and processed. The objective is to define signal processing appropriate for ChemCam data; ultimately, we will be interested to fix the false alarm rate for the detectors. The test statistic is applied to the data set and a decision is made of whether there is signal in the noise based on the threshold. If the signal present decision (D_I) is made, a cost function value is stored to be acted upon by the maximization techniques described later. Note that at least three plasma detections are necessary to optimize the cost function.

The plan to have the ChemCam instrument take reference noise samples of light without firing the laser simplifies the test statistics. The reference signal which is known to contain noise only is used to populate the denominator of each test statistic. Two choices of signal processing are considered:

- 1) Background spectrum white, signal spectrum unknown
- 2) Background spectrum colored, signal spectrum unknown

Option 1 – White Noise

When the background noise is white, the data is reduced to a zero mean by equation 5 with a $\hat{\sigma}^2$ estimated variance. For the Constant False Alarm Rate (CFAR) detector, a reasonable test statistic is the following:

$$T(x_r) = \frac{\frac{1}{N} \sum_{n=0}^{N-1} x_r[n]}{\sqrt{\frac{\hat{\sigma}^2}{N}}} > \gamma \quad (9)$$

Where $T(x_r)$ is the test statistic for the reduced signal plus noise, $x_r[n]$ is obtained from equation 5, γ is the threshold and $\hat{\sigma}^2$ is defined as:

$$\hat{\sigma}^2 = \frac{1}{NM} \sum_{n=0}^{N-1} \sum_{m=0}^{M-1} x_r^2[n, m] \quad (10)$$

where $\hat{\sigma}^2$ is the estimated variance of the noise alone data. An example of the histograms for the test statistic can be found in Figure 35.

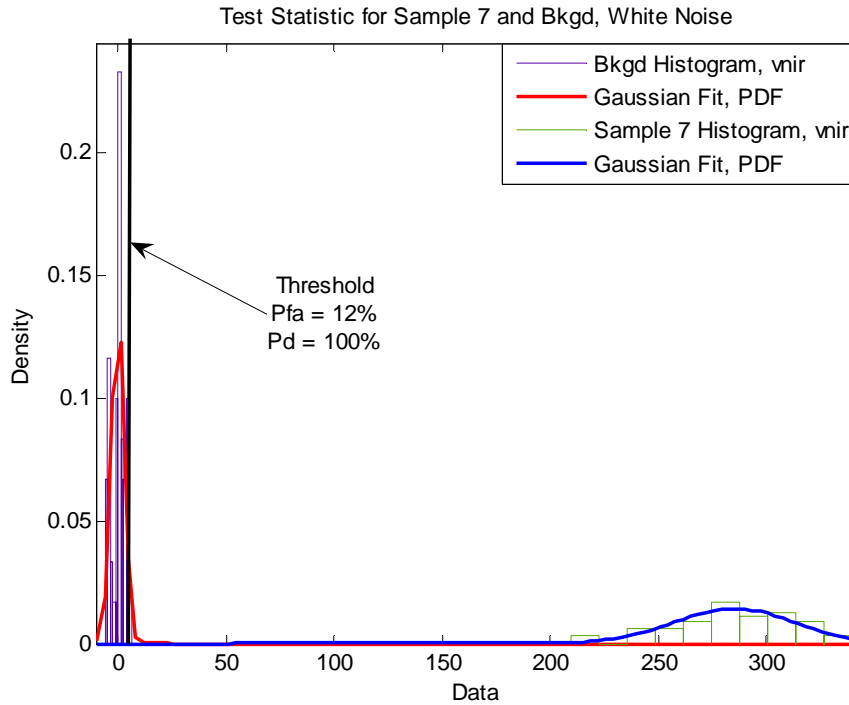


Figure 35 – Histograms of 50 Test Statistics: Sample 7 and Background vnir Spectrometers; Data from Experiment 2

In Figure 35, the histogram for the noise only test statistic is tightly centered on zero due to the subtraction of the mean and the low variance. The Sample 7 test statistic, shown in Figure 35 in the right histogram, has a bigger spread and is shifted substantially in the positive direction. In practice, a threshold is chosen relative to the noise only histogram that fixes the probability of false alarm (P_{FA}) to a value that maximizes the probability of detection (P_D), if possible. In the figure, the threshold is represented by a vertical line that intersects the left histogram. The amount of noise signal content to the right of the threshold determines the P_{FA} (12% for this example). Probabilities are expressed on a percentage basis and a reasonable value to select for P_{FA} is 10% or less. The P_D is determined from the intersection of the signal plus noise histogram with the threshold. The amount of signal content in the signal plus noise histogram to the right of

the threshold is the P_D . As shown in the figure, it is obvious that a threshold chosen as any value between about 20 and 200 will make the P_{FA} 0% and the P_D 100%. In the case of ChemCam, the separation achieved between these histograms would only occur at the closer target distances. The target distances greater than 5 meters will presumably make the threshold much harder to select.

Option 2 – Colored Noise

For colored noise, the development of the detector is similar to the white noise case. The CFAR detector is as follows:

$$T(x_r) = \frac{1}{N} \sum_{n=0}^{N-1} \left(\frac{x_r[n]}{\sqrt{\frac{\hat{\sigma}^2[n]}{N}}} \right) > \gamma \quad (11)$$

But, this time, $x_r[n]$ is obtained from equation 7, consists of the data set from a single laser shot, is normalized by $\hat{\sigma}^2$ in the summation and $\hat{\sigma}^2$ is defined as:

$$\hat{\sigma}^2[n] = \frac{1}{M} \sum_{m=0}^{M-1} (x[n, m] - \mu_r[n])^2 \quad (12)$$

where $\hat{\sigma}^2[n]$ is the estimated variance of each of the 2048 wavelength bins of the 50 background noise shots, $x[n, m]$ is the signal plus noise data and $\mu_r[n]$ is defined by Equation 8. An example of the probability density function (PDF) for the test statistic can be found in Figure 36.

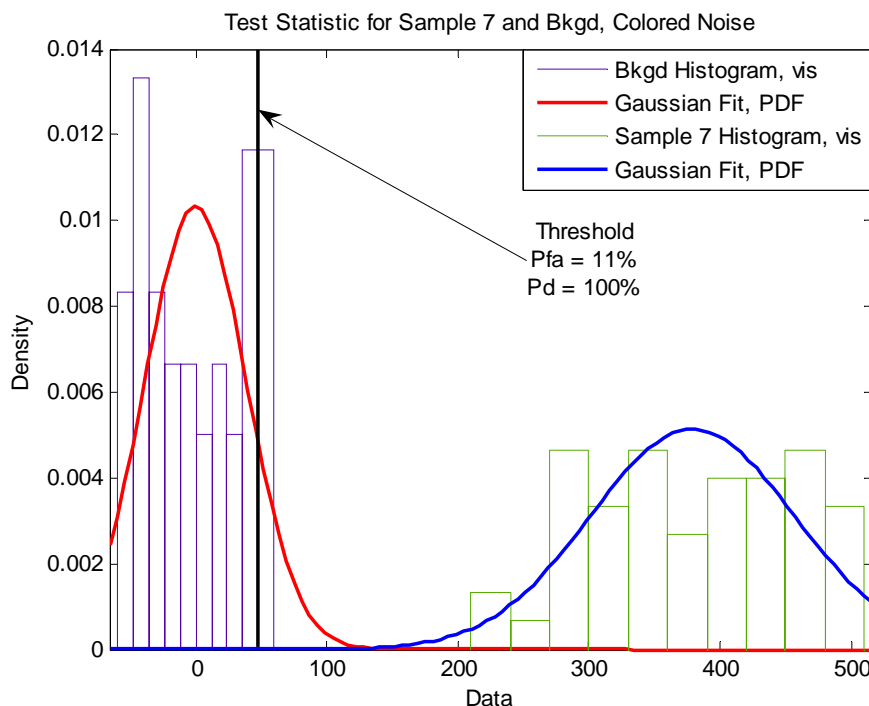


Figure 36 – Histograms of 50 Test Statistics: Sample 7 and Background vis Spectrometers; Data from Experiment 2

In Figure 36, the histogram for the Sample 7 test statistic is the result of performing the data processing described for colored noise. Again, the background noise test statistic is grouped around zero and the threshold is chosen as shown. The threshold value chosen produces a P_{FA} of 11% and a P_D of 100% for the signal plus noise histogram on the right in the figure.

In summary, the signal processing technique depends on the characteristics of the noise, whether colored or white. The two choices detailed in this chapter produce the best results with the ChemCam instrument. Further testing is required to fully implement the detector.

Chapter 5 - Signal Optimization and Computational Analysis

The optimization chosen for this project is a “Golden Section Search in One Dimension” using the motor position as the x and the number of points above threshold as the $f(x)$ [10].

The ChemCam instrument has some computational limitations due to the type of microprocessor, the computational load on the unit and the absence of a math pack to perform mathematical equations. There is also a limit on memory which will necessitate the passing of data to and from the rover computer to perform the laser focusing computations. The algorithms in the appendices are tailored to take advantage of the rover processing power and to limit the burden on ChemCam’s microprocessor.

It is advantageous to analyze the data processing required to quantify the mathematical operations [4]. Several statistical parameters are computed in the algorithm and other parameters are calculated to serve as checks to verify that the equipment and software are operating properly. The maximum, minimum, range, mean, standard deviation, variance and detectability are all computed for each of the spectra (uv, vis and vnir) per the following formulas:

$$max = \max (x[n])$$

where $y[n]$ is the amplitude of light at each pixel and n is the number of pixels.

$$min = \min (x[n])$$

$$R = max - min \tag{17}$$

where R is the range. These metrics are used to determine increasing or decreasing signal content and are computed by making 6,144 comparisons and three subtractions (one for each spectrometer).

$$\mu = \frac{1}{N} \sum_{n=0}^{N-1} x[n] \quad (18)$$

where μ is the arithmetic mean. The mean requires 6,144 additions and three divisions per laser shot.

$$\sigma^2 = \frac{1}{N} \sum_{n=0}^{N-1} (x[n] - \mu)^2 \quad (19)$$

where σ^2 is the variance. The variance requires 6,144 subtractions, 6,144 multiplications and three divisions in addition to the requirements for computing the mean.

$$\sigma = \sqrt{\sigma^2} \quad (20)$$

where σ is the standard deviation. The standard deviation requires three square root calculations.

To capture background noise data for computing the test statistics, the ChemCam instrument will take a number of samples, up to 50 shots without firing the laser. This will require the storage of 307,200 data points. The test statistics require performing mean and variance calculations on these points, similar to the estimates detailed above. However, the background data is crucial to characterizing the baseline data necessary to perform the test statistics. It is not known how long the statistical computations will take the rover computer but a smaller sampling can be proposed.

Conclusion

The methods presented in this thesis project will ensure the focusing of the ChemCam LIBS laser on Mars in day or nighttime operations. Whether searching through a defined target range or through the entire target range of the instrument, the algorithms are robust in their ability to automatically find and optimize plasma light.

Although developed as a backup, these scripts can be implemented as the primary focusing system for the ChemCam laser. If it is decided to implement these algorithms, a period of time is required to debug, test and design the handoffs between the ChemCam microprocessor, the rover computer and the ground system. The scripts are written in MATLAB and an adequate conversion to C is needed prior to implementation.

Appendix A

ChemCam computer commands:

AUTOFOCUSCONFIGURE
AUTOFOCUSGAIN
CONFIGURESTEPPER MOTOR
CONFIGURESTEPPER MOTOR
CONVERTERSWITCHONOFF
GET STARTPOS
GET TARGET
SELECTSPECTROMETERS
STEPPER MOTORLIMITPOINT
STEPPER MOTORMOVE
STEPPER MOTORORCWLONOROFF
TURNONOFFSPECTROMETERS
WARMUPLASER
WARMUPLASERONOFF
XMIT SPECTRA

Appendix B

Software Program for LIBS Laser Focusing (target distance known $\pm 5\%$)

```
% Method 2 Script - Hunt Through Camera Determined Distance Range of
d $\pm$ 0.05d
% This script processes light data obtained from ChemCam
% and controls the instrument to find maximum plasma
% using the signal processing techniques developed by
% Walter C. Barkley, PE
%
% Section 1
% This first section commands the instrument to capture
% background light data in the direction of the laser shot
% (assumes ChemCam is pointed toward the desired target)
% (assumes secondary mirror is at sun-safe position
% (assumes target distance, d is in millimeters
%
% Initialize target distance
d=distance_determined_by_cameras
di=0.95*d;
df=1.05*d;

% Initialize number of motor steps to di and df
ms_initial = -7.053e-19*di^6 + 2.505e-14*di^5 - 3.572e-10*di^4 +2.622e-
06*di^3 - 0.01057*di^2 + 23.09*di - 12940;
ms_final = -7.053e-19*df^6 + 2.505e-14*df^5 - 3.572e-10*df^4 +2.622e-
06*df^3 - 0.01057*df^2 + 23.09*df - 12940;

% Gather three sets of background data without firing the laser to
average for reference noise
% 1st background data set
% Instrument Commands
CONVERTERSWITCHONOFF - on
STEPPERMOTORCWLONOFF - on
CONFIGURESTEPPERMOTOR - input 200
STEPPERMOTORMOVE - input ms_initial
TURNONOFFSPECTROMETERS - on
SELECTSPECTROMETERS - input vnir,vis,uv
XMITSPECTRA - on

% Note: the order of the data stored in B is 1) vnir, 2) vis, 3) uv
% Read and Store Background Data
fid = fopen('textfilename.dat','r');
B1 = fscanf(fid,'%g');
status = fclose(fid);

% Dump the erroneous data
B1(1:50,1)=[];
B1(2049:2148,1)=[];
B1(4097:4196,1)=[];
B1(6145:6194,1)=[];
```



```

% 2nd background data set
TURNONOFFSPECTROMETERS - on
SELECTSPECTROMETERS - input vnir,vis,uv
XMITSPECTRA - on

% Read and Store Background Data
fid = fopen('textfilename.dat','r');
B2 = fscanf(fid,'%g');
status = fclose(fid);

% Dump the erroneous data
B2(1:50,1)=[];
B2(2049:2148,1)=[];
B2(4097:4196,1)=[];
B2(6145:6194,1)=[];

% 3rd background data set
TURNONOFFSPECTROMETERS - on
SELECTSPECTROMETERS - input vnir,vis,uv
XMITSPECTRA - on

% Read and Store Background Data
fid = fopen('textfilename.dat','r');
B3 = fscanf(fid,'%g');
status = fclose(fid);

% Dump the erroneous data
B3(1:50,1)=[];
B3(2049:2148,1)=[];
B3(4097:4196,1)=[];
B3(6145:6194,1)=[];

% Find average
B=(B1+B2+B3)/3;

% Perform statistical measurements of the background
bm_vnir=mean(B(1:2048,1));
bm_vis=mean(B(2049:4096,1));
bm_uv=mean(B(4097:6144,1));

% Shift the background to the origin
bmean1=ones(2048,1)*bm_vnir;
bmean2=ones(2048,1)*bm_vis;
bmean3=ones(2048,1)*bm_uv;
bmean=[bmean1;bmean2;bmean3];
B_shifted=B-bmean;

% Calculate new means and variances
bmean_vnir=mean(B_shifted(1:2048,1));
bmean_vis=mean(B_shifted(2049:4096,1));
bmean_uv=mean(B_shifted(4097:6144,1));

bvar_vnir=var(B_shifted(1:2048,1));

```

```

bvar_vis=var(B_shifted(2049:4096,1));
bvar_uv=var(B_shifted(4097:6144,1));

N=2048;

% Test statistic denominator
d_vnir=sqrt(bvar_vnir/N);
d_vis=sqrt(bvar_vis/N);
d_uv=sqrt(bvar_uv/N);

% Compute thresholds
threshold_vnir=3*sqrt(bvar_vnir);
threshold_vis=3*sqrt(bvar_vis);
threshold_uv=3*sqrt(bvar_uv);

% Section 2
% This section does the data collection and signal processing required
% to determine if there is plasma light present or absent in the
% direction of the target

% Initialize parameters

% Motor step increment
inc=-0.006*d+55;

% Number of laser shots
ls=0.10*d/inc;
IF ls<10
ls=10;
end

% Motor steps per increment and initial motor steps
ms_inc=(ms_initial-ms_final)/ls;

% Data matrices are 6144 X LS
% Capture and store the signal data

% Fire the laser at each increment and collect data
for i=1:ls

% Instrument commands
STEPPERMOTORMOVE - input ms_inc
LASERCONVERTERSONOFF - on
CONFIGURELASERS - input values 1730,1730,1730,100,1,0 (60 Amps) or
CONFIGURELASERS - input values 2878,2878,2878,100,1,0 (100 Amps)
COLLECTSPECTRALIMAGE - input values 330,300,0,255,0,255,0,255,0
XMITSPECTRA - on

% Read and Store Signal Data
fid = fopen('textfilename.dat','r');
C(:,i) = fscanf(fid,'%g');
status = fclose(fid);

```

```

% Dump the erroneous data
C(1:50,i)=[];
C(2049:2148,i)=[];
C(4097:4196,i)=[];
C(6145:6194,i)=[];

% Shift the data toward the origin by the mean of the background
C_shifted(:,i)=C(:,i)-bmean;

% Compute the mean of the data sets
cmean_vnir(i)=mean(C_shifted(1:2048,i));
cmean_vis(i)=mean(C_shifted(2049:4096,i));
cmean_uv(i)=mean(C_shifted(4097:6144,i));

% Compute the range
R_vnir(i)=max(C(1:2048,i))-min(C(1:2048,i));
R_vis(i)=max(C(2049:4096,i))-min(C(2049:4096,i));
R_uv(i)=max(C(4097:6144,i))-min(C(4097:6144,i));

% Compute the test statistics
T_vnir=cmean_vnir(i)/d_vnir;
T_vis=cmean_vis(i)/d_vis;
T_uv=cmean_uv(i)/d_uv;

% Test the hypotheses
count_vnir(i)=FIND(C_shifted(1:2048,i)>T_vnir);
n1(i)=length(count_vnir(i));

count_vis(i)= FIND(C_shifted(2049:4096,i)>T_vis);
n2(i)=length(count_vis(i));

count_uv(i)=FIND(C_shifted(4097:6144,i)>T_uv);
n3(i)=length(count_uv (i));

% Construct x-axis for optimization (number of motor turns)
xms(i)=ms_initial+(i-1)*(ms_inc)

end

% Test cost function
IF n1<3
n2<3
n3<3
OUTPUT: COULD NOT FIND TARGET;
end program

else
% Optimize cost function using Golden Section Search
function [xmax, fmax] = golden(f, ax, bx, cx, tol)

%GOLDEN    Minimize function of one variable using golden section search
%
```

```

% [xmax, fmax] = golden(f, ax, bx, cx, tol) computes a local maximum
% of f. xmax is the computed local maximizer of f and fmax is
% f(xmax). xmax is computed to a relative accuracy of TOL.
%
% The parameters ax, bx and cx must satisfy the following conditions:
% ax < bx < cx, f(bx) > f(ax) and f(bx) > f(cx).
%
% xmax satisfies ax < xmax < cx. Golden is guaranteed to succeed if f
% is continuous between ax and cx
%
c = (3-sqrt(5))/2;
r = 1-c;

x0 = ax;
x3 = cx;
if (abs(cx-bx) > abs(bx-ax)),
    x1 = bx;
    x2 = bx + C*(cx-bx);
else
    x2 = bx;
    x1 = bx - C*(bx-ax);
end
f1 = feval(f,x1);
f2 = feval(f,x2);

k = 1;
while abs(x3-x0) > tol*(abs(x1)+abs(x2)),
    fprintf(1,'k=%4d, |a-b|=%e\n', k, abs(x3-x0));
    if f2 < f1,
        x0 = x1;
        x1 = x2;
        x2 = R*x1 + C*x3;    % x2 = x1+c*(x3-x1)
        f1 = f2;
        f2 = feval(f,x2);
    else
        x3 = x2;
        x2 = x1;
        x1 = R*x2 + C*x0;    % x1 = x2+c*(x0-x2)
        f2 = f1;
        f1 = feval(f,x1);
    end
    k = k+1;
end

if f1 < f2,
    xmin = x1;
    fmin = f1;
else
    xmin = x2;
    fmin = f2;
end

end

```

Appendix C

Software Program for LIBS Laser Focusing (target distance unknown)

```
% Method 1 Script - Hunt Through Entire Range of LIBS Laser
% This script processes light data obtained from ChemCam
% and controls the instrument to find maximum plasma
% using the signal processing techniques developed by
% Walter C. Barkley, PE
%
% Section 1
% This first section commands the instrument to capture
% background light data in the direction of the laser shot
% (assumes ChemCam is pointed toward the desired target)
% (assumes secondary mirror is at sun-safe position
% (assumes target distance, d is in millimeters
%
% Initial and final target distances (mm)
di=1500;
df=9000;

% Initialize number of motor steps to di and df
ms_initial = -7.053e-19*di^6 + 2.505e-14*di^5 - 3.572e-10*di^4 +2.622e-
06*di^3 - 0.01057*di^2 + 23.09*di - 12940;
ms_final = -7.053e-19*df^6 + 2.505e-14*df^5 - 3.572e-10*df^4 +2.622e-
06*df^3 - 0.01057*df^2 + 23.09*df - 12940;

% Gather three sets of background data to average
% 1st background data set
% Instrument Commands
CONVERTERSWITCHONOFF - on
STEPPERMOTORCWLONOFF - on
CONFIGURESTEPPERMOTOR - input 200
STEPPERMOTORMOVE - input ms_initial
TURNONOFFSPECTROMETERS - on
SELECTSPECTROMETERS - input vnir,vis,uv
XMITSPECTRA - on

% Note: the order of the data stored in B is 1) vnir, 2) vis, 3) uv
% Read and Store Background Data
fid = fopen('textfilename.dat','r');
B1 = fscanf(fid,'%g');
status = fclose(fid);

% Dump the erroneous data
B1(1:50,1)=[];
B1(2049:2148,1)=[];
B1(4097:4196,1)=[];
B1(6145:6194,1)=[];

% 2nd background data set
TURNONOFFSPECTROMETERS - on
SELECTSPECTROMETERS - input vnir,vis,uv
```

```

XMIT SPECTRA - on

% Read and Store Background Data
fid = fopen('textfilename.dat','r');
B2 = fscanf(fid,'%g');
status = fclose(fid);

% Dump the erroneous data
B2(1:50,1)=[];
B2(2049:2148,1)=[];
B2(4097:4196,1)=[];
B2(6145:6194,1)=[];

% 3rd background data set
TURNONOFFSPECTROMETERS - on
SELECTSPECTROMETERS - input vnir,vis,uv
XMIT SPECTRA - on

% Read and Store Background Data
fid = fopen('textfilename.dat','r');
B3 = fscanf(fid,'%g');
status = fclose(fid);

% Dump the erroneous data
B3(1:50,1)=[];
B3(2049:2148,1)=[];
B3(4097:4196,1)=[];
B3(6145:6194,1)=[];

% Find average
B=(B1+B2+B3)/3;

% Perform statistical measurements of the background
bm_vnir=mean(B(1:2048,1));
bm_vis=mean(B(2049:4096,1));
bm_uv=mean(B(4097:6144,1));

% Shift the background to the origin
bmean1=ones(2048,1)*bm_vnir;
bmean2=ones(2048,1)*bm_vis;
bmean3=ones(2048,1)*bm_uv;
bmean=[bmean1;bmean2;bmean3];
B_shifted=B-bmean;

% Calculate new means and variances
bmean_vnir=mean(B_shifted(1:2048,1));
bmean_vis=mean(B_shifted(2049:4096,1));
bmean_uv=mean(B_shifted(4097:6144,1));

bvar_vnir=var(B_shifted(1:2048,1));
bvar_vis=var(B_shifted(2049:4096,1));
bvar_uv=var(B_shifted(4097:6144,1));

```

```

N=2048;

% Test statistic denominator
d_vnir=sqrt(bvar_vnir/N);
d_vis=sqrt(bvar_vis/N);
d_uv=sqrt(bvar_uv/N);

% Compute thresholds
threshold_vnir=3*sqrt(bvar_vnir);
threshold_vis=3*sqrt(bvar_vis);
threshold_uv=3*sqrt(bvar_uv);

% Section 2
% This section does the data collection and signal processing required
% to determine if there is plasma light present or absent in the
% direction of the target

% Initialize parameters

% split distance range into three segments and take midpoint:
% 1500-2000mm, 2001-5000mm, 5001-9000mm
dt=[1750; 2500; 7500];

% Motor step increment
Inc=[45; 27.5; 10];

% Number of laser shots
ls=dt./inc;

% Motor steps per increment and initial motor steps
ms_inc=(ms_initial-ms_final)./ls;

% Data matrices are 6144 X LS
% Capture and store the signal data

% Fire the laser at each increment and collect data
for i=1:ls

% Instrument commands
STEPPERMOTORMOVE - input ms_inc
LASERCONVERTERSONOFF - on
CONFIGURELASERS - input values 1730,1730,1730,100,1,0 (60 Amps) or
CONFIGURELASERS - input values 2878,2878,2878,100,1,0 (100 Amps)
COLLECTSPECTRALIMAGE - input values 330,300,0,255,0,255,0,255,0
XMITSPECTRA - on

% Read and Store Signal Data
fid = fopen('textfilename.dat','r');
C(:,i) = fscanf(fid,'%g');
status = fclose(fid);

% Dump the erroneous data
C(1:50,i)=[];

```

```

C(2049:2148,i)=[];
C(4097:4196,i)=[];
C(6145:6194,i)=[];

% Shift the data toward the origin by the mean of the background
C_shifted=C-bmean;

% Compute the mean of the data sets
cmean_vnir(i)=mean(C_shifted(1:2048,i));
cmean_vis(i)=mean(C_shifted(2049:4096,i));
cmean_uv(i)=mean(C_shifted(4097:6144,i));

% Compute the range
R_vnir(i)=max(C(1:2048,i))-min(C(1:2048,i));
R_vis(i)=max(C(2049:4096,i))-min(C(2049:4096,i));
R_uv(i)=max(C(4097:6144,i))-min(C(4097:6144,i));

% Compute the test statistics
T_vnir=cmean_vnir(i)/d_vnir;
T_vis=cmean_vis(i)/d_vis;
T_uv=cmean_uv(i)/d_uv;

% Test the hypotheses
count_vnir(i)=FIND(C_shifted(1:2048,i)>T_vnir);
n1(i)=length(count_vnir(i));

count_vis(i)= FIND(C_shifted(2049:4096,i)>T_vis);
n2(i)=length(count_vis(i));

count_uv(i)=FIND(C_shifted(4097:6144,i)>T_uv);
n3(i)=length(count_uv (i));

% Construct x-axis for optimization (number of motor turns)
xms(i)=ms_initial+(i-1)*(ms_inc)

end

% Test cost function
IF n1<3
n2<3
n3<3
OUTPUT: COULD NOT FIND TARGET;
end program

else
% Optimize cost function using Golden Section Search
function [xmax, fmax] = golden(f, ax, bx, cx, tol)

%GOLDEN    Minimize function of one variable using golden section search

```



```

%
% [xmax, fmax] = golden(f, ax, bx, cx, tol) computes a local maximum
% of f. xmax is the computed local maximizer of f and fmax is
% f(xmax). xmax is computed to a relative accuracy of TOL.
%
% The parameters ax, bx and cx must satisfy the following conditions:
% ax < bx < cx, f(bx) > f(ax) and f(bx) > f(cx).
%
% xmax satisfies ax < xmax < cx. Golden is guaranteed to succeed if f
% is continuous between ax and cx
%
c = (3-sqrt(5))/2;
r = 1-c;

x0 = ax;
x3 = cx;
if (abs(cx-bx) > abs(bx-ax)),
    x1 = bx;
    x2 = bx + C*(cx-bx);
else
    x2 = bx;
    x1 = bx - C*(bx-ax);
end
f1 = feval(f,x1);
f2 = feval(f,x2);

k = 1;
while abs(x3-x0) > tol*(abs(x1)+abs(x2)),
    fprintf(1,'k=%4d, |a-b|=%e\n', k, abs(x3-x0));
    if f2 < f1,
        x0 = x1;
        x1 = x2;
        x2 = R*x1 + C*x3;    % x2 = x1+c*(x3-x1)
        f1 = f2;
        f2 = feval(f,x2);
    else
        x3 = x2;
        x2 = x1;
        x1 = R*x2 + C*x0;    % x1 = x2+c*(x0-x2)
        f2 = f1;
        f1 = feval(f,x1);
    end
    k = k+1;
end

if f1 < f2,
    xmin = x1;
    fmin = f1;
else
    xmin = x2;
    fmin = f2;
end

end

```

References

- [1] http://mars.jpl.nasa.gov/msl/mission/Rover_Update.html
- [2] Cremers, David A. et al, *LIBS Analysis of Geological Samples at Low Pressures: Application to Mars, the Moon and Asteroids*, Los Alamos National Laboratory Publication, LA-UR-04-0548, 2005
- [3] http://libs.lanl.gov/ChemCam_Art_Open.html
- [4] Bewley, Thomas, *Numerical Renaissance*, 2008
- [5] <http://nssdc.gsfc.nasa.gov/planetary/factsheet/marsfact.htm>
- [6] Emsley, John, *The Elements*, 1998
- [7] <http://www.brammerstandard.com/>
- [8] Kay, Steven, *Fundamentals of Statistical Signal Processing, Volume II: Detection Theory*, 1998
- [9] Kay, Steven, *Fundamentals of Statistical Processing, Volume I: Estimation Theory*, 1993
- [10] Press, William H, et al, *Numerical Recipes in C*, 1988